Biotechnology Advances 43 (2020) 107583

Contents lists available at ScienceDirect

Biotechnology Advances

journal homepage: www.elsevier.com/locate/biotechadv

Research review paper

Heterologous expression of lytic polysaccharide monooxygenases (LPMOs)

Yasser Gaber[a,b], Boshra Rashad[c], Rasha Hussein[b,d], Mai Abdelgawad[c], Nourhan S. Ali[c], Tarek Dishisha[a], Anikó Várnai[e,*]

[a] Department of Microbiology and Immunology, Faculty of Pharmacy, Beni-Suef University, Beni-Suef 62511, Egypt
[b] Department of Pharmaceutics and Pharmaceutical Technology, College of Pharmacy, Mutah University, Al-Karak 61710, Jordan
[c] Biotechnology and Life Sciences Department, Faculty of Postgraduate Studies for Advanced Sciences (PSAS), Beni-Suef University, Beni-Suef 62511, Egypt
[d] Department of Biochemistry, Faculty of Pharmacy, Beni-Suef University, Beni-Suef 62511, Egypt
[e] Faculty of Chemistry, Biotechnology and Food Science, Norwegian University of Life Sciences, Ås 1430, Norway

ARTICLE INFO

Keywords:
LPMOs
Protein expression
Auxiliary activity
Expression vector
Signal peptide
Protein tag
Post-translational modifications
Active-site copper
Culture conditions

ABSTRACT

Lytic polysaccharide monooxygenases (LPMOs) are relatively new enzymes that have been discovered 10 years ago. LPMOs comprise a diverse group of enzymes which play a pivotal role in the depolymerization of sugar-based biopolymers including cellulose, hemicellulose, chitin, and starch. Their mechanism of action relies on the correct coordination of a copper ion in the active site, which is partly composed of the N-terminal histidine. Therefore, correct secretion and folding of these copper-enzymes is fundamental for obtaining a catalytic activity. LPMOs occur in all kingdoms of life; they have been found in viruses, bacteria and eukaryotes, including fungi, plants and animals. In many cases, using homologous expression of these proteins is not feasible and an alternative organism, which can be cultured and is able to heterologously express the protein of interest, is required for studying enzyme properties. Therefore, we made an extensive compilation of expression techniques used for LPMOs the expression and characterization of which have been reported to date. In the current review, we provide a summary of the different techniques, including expression hosts and vectors, secretion methods, and culturing conditions, that have been used for the overexpression and production of this important class of enzymes at laboratory scale. Herein, we compare these techniques and assess their advantages and disadvantages.

1. Background

Oxidative cleavage of polysaccharides by lytic polysaccharide monooxygenases (LPMOs) have been discovered in the past decade (Vaaje-Kolstad et al., 2010), and shortly thereafter, the structure of the LPMOs' copper loaded active site has been elucidated (Quinlan et al., 2011). Since then, LPMOs have been subjected to different nomenclature and classification along the way based on the state of knowledge of the mechanism attributed to these proteins. While the exact mechanism of LPMO-mediated polysaccharide oxidation is still under debate to date (Bissaro et al., 2017; Walton and Davies, 2016), five EC Numbers, namely EC 1.14.99.53-56 and 1.14.99.B10, have been assigned so far to LPMO action in the Enzyme Commission classification system (McDonald et al., 2009). LPMOs have also been classified in the Carbohydrate-Active enZymes (CAZy) database (Levasseur et al., 2013), within the Auxiliary Activity (AA) families AA9-11 and AA13-16, on account of their activity on polysaccharides. These enzymes share an immunoglobulin-like β-sandwich fold in the core of the protein, a copper atom coordinated by a His-brace in the catalytic center (Quinlan et al., 2011), and the ability to cleave various polysaccharides (Agger

Abbreviations: *A. nidulans*, *Aspergillus nidulans*; *A. oryzae*, *Aspergillus oryzae*; AA, Auxiliary Activity; *B. amyloliquefaciens*, *Bacillus amyloliquefaciens*; *B. atrophaeus*, *Bacillus atrophaeus*; *B. licheniformis*, *Bacillus licheniformis*; *B. subtilis*, *Bacillus subtilis*; *E. coli*, *Escherichia coli*; *F. fujikuroi*, *Fusarium fujikuroi*; *G. candidum*, *Geotrichum candidum*; *H. jecorina*, *Hypocrea jecorina*; IPTG, isopropyl-β-D-thiogalactopyranoside; LPMO, lytic polysaccharide monooxygenase; *M. thermophila*, *Myceliophthora thermophila*; *N. crassa*, *Neurospora crassa*; *P. chrysosporium*, *Phanerochaete chrysosporium*; *P. pastoris*, *Pichia pastoris*; *P. verruculosum*, *Penicillium verruculosum*; PTM, post-translational modification; *S. cerevisiae*, *Saccharomyces cerevisiae*; *S. coelicolor*, *Streptomyces coelicolor*; *S. elongatus*, *Synechococcus elongatus*; *S. lividans*, *Streptomyces lividans*; *S. marcescens*, *Serratia marcescens*; *T. aurantiacus*, *Thermoascus aurantiacus*; *T. cellulolyticus*, *Talaromyces cellulolyticus*; *T. domestica*, *Thermobia domestica*; *T. fusca*, *Thermobifida fusca*; *T. reesei*, *Trichoderma reesei*; *T. turnerae*, *Teredinibacter turnerae*; *Y. lipolytica*, *Yarrowia lipolytica*.

* Corresponding author at: Faculty of Chemistry, Biotechnology and Food Science, Norwegian University of Life Sciences (NMBU), PO Box 5003, 1432 Ås, Norway.
E-mail addresses: Yasser.Gaber@pharm.bsu.edu.eg (Y. Gaber), BoshraMohamed@psas.bsu.edu.eg (B. Rashad), Rasha.Hussein@pharm.bsu.edu.eg (R. Hussein), MaiAli@psas.bsu.edu.eg (M. Abdelgawad), Nourhan200@gmail.com (N.S. Ali), Tarek.Dishisha@pharm.bsu.edu.eg (T. Dishisha), Aniko.Varnai@nmbu.no (A. Várnai).

https://doi.org/10.1016/j.biotechadv.2020.107583
Received 19 December 2019; Received in revised form 19 June 2020; Accepted 20 June 2020
Available online 04 July 2020

et al., 2014; Forsberg et al., 2011; Frommhagen et al., 2015; Vaaje-Kolstad et al., 2010).

While the first enzymes characterized as LPMOs were of bacterial (CBP21 or *Sm*AA10A from *Serratia marcescens* (Vaaje-Kolstad et al., 2010)) and fungal (*Ta*GH61 or *Ta*AA9A from *Thermoascus aurantiacus* (Quinlan et al., 2011)) origins, to date, LPMOs are known to be present in all kingdoms of life: bacteria (AA10), archaea (AA10), fungi (AA9-11, AA13-14, AA16), protists (AA10, AA15), plants (AA10) and animals (AA15), as well as in viruses (AA10, AA15) (Levasseur et al., 2013). Although AA10 LPMOs have been found in most kingdoms of life, AA10 LPMOs occur predominantly in non-eukaryotic organisms, with bacteria and viruses comprising 96% and 3% of AA10s reported as of today in the CAZy database, respectively. As underlined by their wide occurrence, LPMOs function in various environments and have various biological roles, including polysaccharide metabolism (Kracher et al., 2016), virulence (Garcia-Gonzalez et al., 2014; Wong et al., 2012), and insect development (Sabbadin et al., 2018). In addition, LPMOs may be subjected to various post-translational modifications depending on their origin with effects on protein function and stability. Consequently, selecting the right expression platform is critical to obtain functional proteins.

A number of reviews have discussed LPMOs recently in terms of their mechanism (Bissaro et al., 2018; Chylenski et al., 2019; Tandrup et al., 2018; Walton and Davies, 2016), 3D structure (Lo Leggio et al., 2012; Vaaje-Kolstad et al., 2017; Vu and Ngo, 2018), as well as biochemical (Eijsink et al., 2019) and spectroscopic characterization (Hemsworth et al., 2018). Lately, Hemsworth et al. (2018) presented a brief overview of the most common expression platforms for LPMOs. In the current review, we aim to complement these aspects by providing a comprehensive summary of the methods that have been used for expression of LPMOs for structural and biochemical characterization and biotechnological application. This review presents a critical assessment of considerations that need to be carefully made in order to select a suitable approach for successful expression of a functional LPMO.

In the following sections, we will provide an overview of LPMO structure and function which are relevant to the selection of expression platform and design of cloning of so far uncharacterized LPMOs. Subsequently, we will present the expression platforms used for expressing LPMOs of various origins and assess the advantages and disadvantages of these expression platforms with regards to their impact on protein stability and biochemical activity. Then, we will discuss the impact of culture conditions on the production of active LPMOs in connection with the current status of LPMO production at bioreactor scale. Finally, we will address strategies for scaling up LPMO production successfully regarding the exploitation of these enzymes for various biotechnological applications at industrial scale.

2. Structural features of LPMOs important for functionality

LPMOs share an immunoglobulin-like β-sandwich fold irrespective of the organism of origin (Chiu et al., 2015; Karkehabadi et al., 2008; Sabbadin et al., 2018; Vaaje-Kolstad et al., 2005). Correct protein folding relies on the formation of disulfide bridges, which are essential for thermodynamic stability (Tanghe et al., 2017). Furthermore, LPMOs (Fig. 1) possess a distinct catalytic site, comprised of a His-pair (so-called His-brace) coordinating a copper ion (Quinlan et al., 2011). The presence of copper in the active site is important for stability, which is indicated by a decrease in melting temperature upon removal of the copper (Hemsworth et al., 2013a; Kracher et al., 2018; Sabbadin et al., 2018). The His-brace has a high affinity (in the nM range) to copper (Aachmann et al., 2012), which ensures that free copper will be incorporated into the catalytic site from the culture medium during protein production as well as from the buffer solution or substrate in the reaction setup unless chelated with EDTA and other chelating agents.

One of the two catalytic His is located at the N-terminus, and the α-amino group of the N-terminal His1 takes part in the coordination of the active-site copper (Fig. 1). Consequently, the protein has to be secreted (to the extracellular or, in case of Gram-negative bacteria, the periplasmic space), and obtaining a functional catalytic site can be hindered by incorrect processing of the signal peptide. Intriguingly, the N-terminal His has been found methylated in AA9 LPMOs expressed in filamentous fungi (Quinlan et al., 2011). While such a modification at the catalytic site indicates a role in the catalytic mechanism, AA9 LPMOs expressed in yeast and bacterial AA10 LPMOs are also active despite lacking methylation of the His1. Quinlan et al. (2011) noted that the methylation could modulate the reactivity of the active site copper. Later, based on the X-ray structure of an LPMO-cellotriose complex, Frandsen et al. (2016) postulated that the methylation of His1 facilitates substrate binding via stabilizing the electrostatic interaction of the imidazole ring of His1 with the sugar residue residing at the subsite +1 (Frandsen et al., 2016; Simmons et al., 2017). On the other hand, Kim et al. (2014) predicted that the methylation has an insignificant effect on the LPMO catalytic activity based on quantum-mechanical modeling. Recently, Petrović et al. (2018) reported the functional comparison of the methylated and non-methylated variants of *Ta*AA9A from *T. aurantiacus*. The authors showed that methylation of the His1 (as well as the difference in the glycosylation pattern by the distinct expression hosts) had no impact on the LPMO's affinity for copper, the redox potential of bound copper, substrate preference, cleavage specificity or the ability to activate molecular oxygen. On the other hand, the methylated variant had increased redox stability, was more resistant to excess H_2O_2, and performed better in an applied setting. While the authors found strong indications regarding the protective role of methylation against oxidative damage of the active-site residues, it cannot be excluded that the difference in glycosylation pattern may have substantially contributed to the observed difference in protein stability. The exact role of the methyl group in the catalytic reaction, as of today, remains elusive.

3. Heterologous expression of LPMOs

In the age of bioprospecting, homologous expression is not always feasible when producing proteins for characterization and biotechnological applications. In several cases, the source organism cannot be cultured *in vitro* and/or LPMOs cannot be produced/isolated (at all or in large enough quantities for characterization and biotechnological application). Moreover, enzyme production for industrial applications requires expression hosts with which production can be easily scaled up and enzymes can be obtained in high concentration and, depending on the desired application, in a relatively pure form. Therefore, alternative organisms need to be selected for heterologous expression, with the prerequisite to produce catalytically active LPMOs. Although the common protein fold of LPMOs indicates that heterologous expression of these proteins is likely to succeed in the most common bacterial and fungal expression hosts, aspects related to exon-intron recognition (in eukaryotic systems), similarity in secretion pathways (for signal peptide recognition) and differences in post-translational modifications in the native and expression hosts need to be considered. These issues are addressed below.

3.1. The choice of expression host and vector

3.1.1. Expression of bacterial LPMOs

In general, bacterial (prokaryotic) LPMOs are commonly expressed using the Gram-negative bacterium *Escherichia coli* (Table 1 and Supplementary Table S1) via periplasmic expression (Fig. 2A). Among the different *E. coli* strains, BL21(DE3) and its derivatives C43(DE3), BL21(DE3)pLysS, and pLysE have been used for LPMO expression, in conjunction with the pRSET and pET vectors. BL21(DE3) strains have the bacteriophage T7 RNA polymerase incorporated in their chromosome, and upon induction with isopropyl-β-D-thiogalactopyranoside (IPTG), the T7 RNA polymerase is expressed and transcribes the target

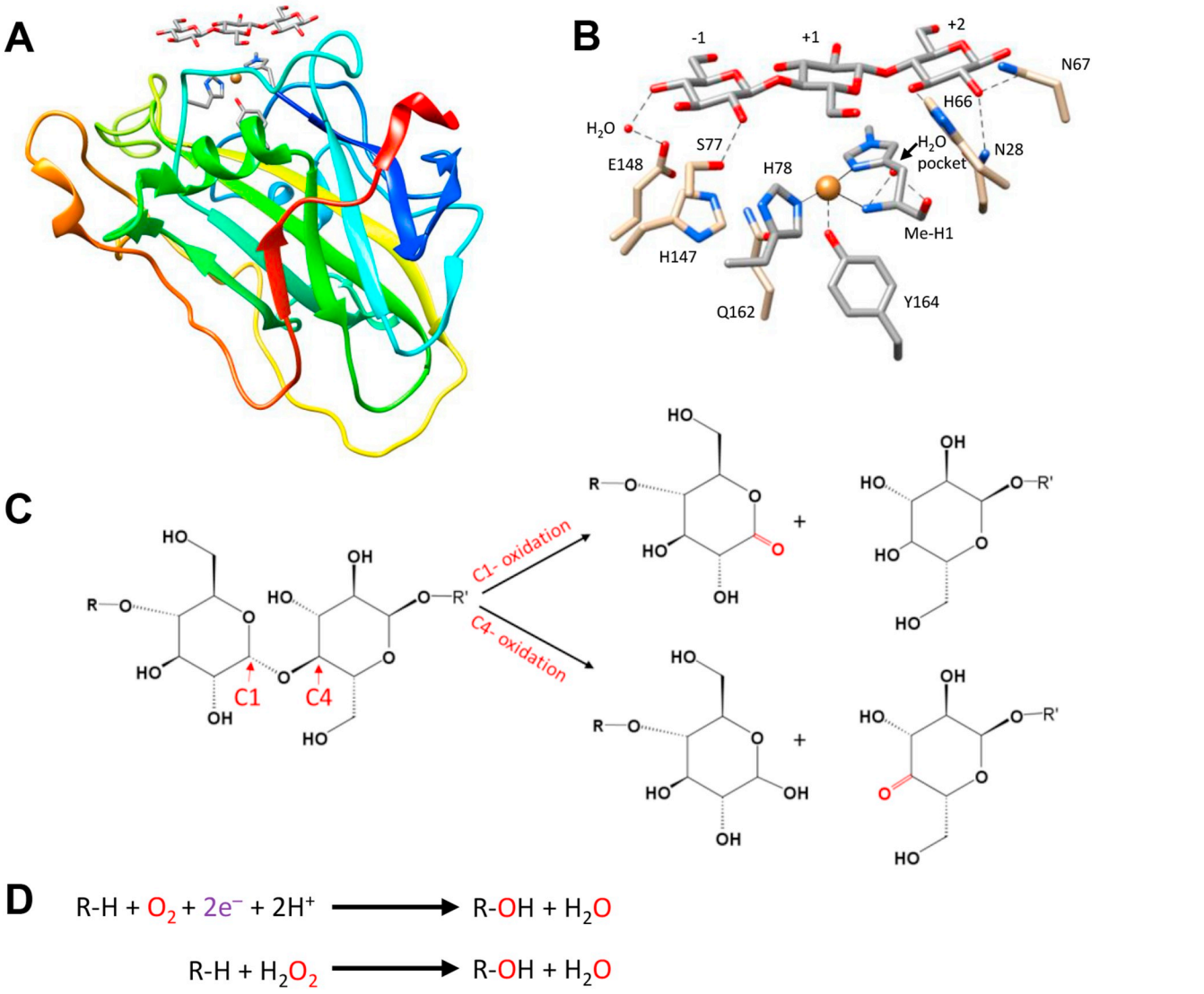

Fig. 1. Three-dimensional structure and catalytic mechanism of a typical LPMO. (A) Crystal structure of *Ls*AA9A, an LPMO from *Lentinus similis*, with cellotriose bound at the active site (PDB ID, 5ACF). (B) A close-up view of the active site structure with cellotriose, showing the amino acid residues that take part in copper coordination and substrate binding (Frandsen et al., 2016). The copper atom, coordinated by His1, His78 and Tyr164, is shown as a golden sphere. Gln162 near the active site copper is highly conserved (Gln/Glu) and is likely to take part in the stabilization of H_2O_2 during the catalytic cycle (Bissaro et al., 2020; Wang et al., 2019). (C) Oxidative cleavage of cellulose by LPMOs, showing cleavage upon hydroxylation at the C-1 or C-4 carbon by the LPMO. Depending on the regioselectivity, LPMOs generate only C1- or C4-oxidized chain ends or a mixture of both. (D) General reaction schemes for the two proposed LPMO reaction mechanisms driven by either O_2 or H_2O_2 as co-substrates (Bissaro et al., 2017; Vaaje-Kolstad et al., 2010).

gene located on the expression vector under the control of the strong phage T7 promoter. Despite the stringent repression of the T7 promoter, basal expression of the T7 RNA polymerase and hence production of the target protein occur even before addition of IPTG. LPMO production has often been observed even without induction with IPTG (Forsberg et al., 2018; Vaaje-Kolstad et al., 2005). Several strategies have been developed to ensure tight control, which is necessary in case of proteins that may be toxic to the expression host. BL21(DE3)pLysS and pLysE strains express the T7 lysozyme, which binds to the T7 RNA polymerase and thereby represses transcription of the target gene (Huang et al., 1999). In addition, some of the pET vectors carry the T7*lac* promoter and encode an additional *lac* repressor, which represses transcription of the T7 RNA polymerase and blocks transcription of the target gene. Protein production is induced with IPTG, which binds to the *lac* repressor. Notably, the T7 RNA polymerase system is suboptimal for producing isotopically labelled LPMOs, e.g. for NMR experiments (Courtade et al., 2017)), as glucose in the defined production media will repress T7 RNA polymerase concentration and lower LPMO yield. To overcome catabolite repression, Courtade et al. (2017) developed the pJB and pJB_SP vectors (the latter including the signal peptide of *Sm*AA10A from *S. marcescens*) based on the pGM29 vector harboring the XylS/*Pm* regulator/promoter system, with *m*-toluic acid as inducer.

The Gram-positive bacterium *Bacillus subtilis* has also been used as expression host for the production of an AA10 LPMO from *Bacillus atrophaeus* (Yu et al., 2016). *B. subtilis* has naturally high secretion capacity and secretes proteins directly into the extracellular medium. In contrast to *E. coli*, however, little is known about disulfide bond formation (Westers et al., 2004). Limitations in protein expression due to low plasmid stability and difficulty in the transformation and protoplast preparation have been improved lately (Nguyen et al., 2005). Moreover, the availability of protease-deficient strains such as *B. subtilis* LKS87 (DB104, *amyE*, *his*$^+$, *nprR*$_2$, *nprR*$_{12}$, Δ*aprA*$_3$), which has been used for LPMO production (Yu et al., 2016), improves the stability of the target protein during production. Moreover, since the original gene encoding the LPMO derives from another species in the *Bacillus* genus, the authors have been able to utilize the native signal peptide and the *B.*

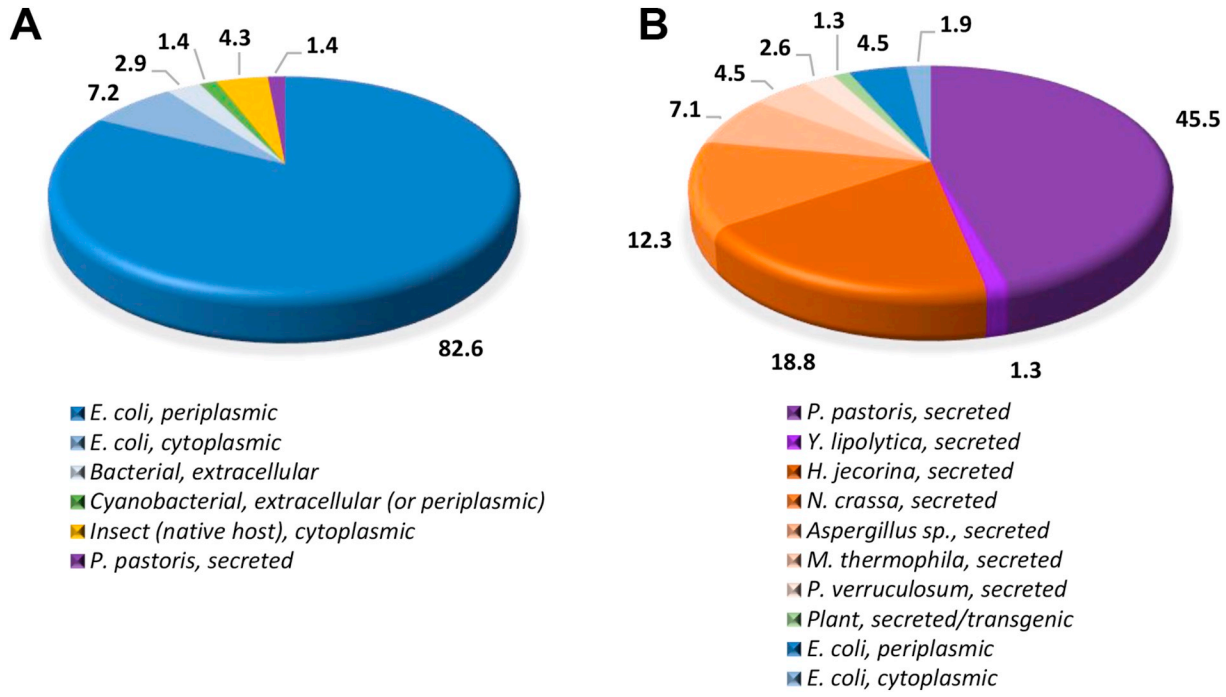

Fig. 2. The relative percentages of the use of different expression strategies for the production of A) bacterial and viral LPMOs and B) Eukaryotic LPMOs. Relative percentages were calculated based on 69 entries of bacterial and viral LPMOs and 154 entries of fungal, yeast, insect, and plant LPMOs, as indicated in Supplementary Table S1.

subtilis secretion system, without the need for induction of protein expression. This has resulted in several benefits including improved productivity and relatively easy downstream processing for purification as compared with periplasmic expression in *E. coli*.

Very recently, Russo et al. (2019) have demonstrated heterologous expression of an LPMO from the Gram-positive bacterium *Thermobifida fusca* in the cyanobacterium *Synechococcus elongatus* UTEX 2973. The major advantages of using *S. elongatus* as expression host are that it is fast-growing and genetically tractable, and, being a cyanobacterium, it can grow on cheap inorganic nutrients and CO_2. *Tf*AA10A from *T. fusca* has been expressed successfully with correctly processed N-terminus using the native Sec-targeting signal peptide of the LPMO, although with low yield (< 1 mg/L). When using the endogenous Tat-targeting TorA signal peptide instead of the native one, the LPMO has been found unprocessed in the plasma membrane. While cyanobacteria have a growing potential as cell factories in consolidated bioprocessing, their application for the production of individual enzymes has been limited so far.

It is noteworthy that bacterial enzymes from extremophiles and organisms from marine sources are often misfolded upon synthesis, leading to protein aggregation and formation of inclusion bodies when expressed in *E. coli*. Chaperones assist protein folding and have been shown to facilitate overexpression of recombinant proteins in *E. coli* (Haacke et al., 2009). Chaperon-assisted protein folding may also be considered when overexpressing LPMOs from bioprospecting studies. Accordingly, it has been successfully applied in one study, when expressing an AA10 from the shipworm symbiont *Teredinibacter turnerae* (Fowler et al., 2019). The LPMO domain of *Tt*AA10A has been produced in *E. coli* transformed with the pGro7 chaperone plasmid, after multiple unsuccessful attempts using a variety of solubility and affinity tags and secretion signals.

3.1.2. Expression of LPMOs from fungi, higher Eukaryotes, and viruses

Eukaryotic (primarily fungal) LPMOs, on the other hand, are most commonly expressed with eukaryotic expression hosts such as the yeast *Pichia pastoris* or the filamentous fungi *Hypocrea jecorina* (formerly *Trichoderma reesei*), *Neurospora crassa*, *Aspergillus oryzae* and *Myceliophthora thermophila*, using species-specific cloning vectors (Table 1, Fig. 2B, and Supplementary Table S1). Notably, many of these fungal strains are industrial strains used for the production of biomass-degrading enzyme cocktails and are heavily engineered, cellulase-deficient derivatives of native strains (Aehle et al., 2009; Dotson et al., 2007; Makinen et al., 2014; Punt et al., 2010). Alternatively to heterologous expression, LPMOs have, in some cases, also been isolated from the native host (or its engineered derivative), such as the *M. thermophila* C1 strain (Frommhagen et al., 2016; Visser et al., 2011). A major advantage of using eukaryotic expression systems over bacterial expression systems is that in eukaryotic expression systems the gene of interest is incorporated in the chromosomal DNA; hence, there is no need for a selection marker (i.e. to retain the plasmid carrying the gene of interest) after a production strain has been selected. When expressing LPMOs from filamentous fungi, further advantages include recognition and correct processing of the native LPMO signal peptide, secretion of the target protein into the extracellular space, methylation of the N-terminal histidine (Petrović et al., 2018; Quinlan et al., 2011), similar-to-native glycosylation of the linker peptide of multidomain LPMOs and good protein yield, as detailed further below.

A. oryzae is the most common filamentous fungus used as a fungal expression host, and several *A. oryzae* strains, including JaL250, JaL355, MSTR212 and MT3568, have been employed for LPMO production (Frandsen et al., 2017; Frandsen et al., 2016; Lo Leggio et al., 2015; Quinlan et al., 2011; Simmons et al., 2017). The target gene is usually expressed under the control of a host promoter using the native signal peptide (Fitz et al., 2018). This results in a high background of CAZymes in the broth (as plant cell wall-active CAZymes are co-regulated under a set of promoters), demanding a more complicated purification method. Strategies to reduce background activities include the use of multiple knockout strains (Visser et al., 2011) or expression under synthetic expression system in cellulase-repressing glucose medium (Rantasalo et al., 2019). However, at the moment, fungal expression systems are not readily available on the market, working with them is time-consuming, and, even with the recently developed

Table 1
Protein expression systems used for LPMO production. A complete list of expression strategies used for LPMO expression can be found in Supplementary Table S1.

CAZy family	Expression strain	Localization	Expression vector	Secretion signal	Gene source	Examples
AA9	*Fungal expression systems*					
	A. oryzae JaL250	Extracellular	pAILo2	Native	Genomic DNA	*Tt*AA9E from *Thielavia terrestris* (Harris et al., 2010); *Ta*AA9A from *T. aurantiacus* (Quinlan et al., 2011)
	H. jecorina / T. reesei Δ(*cbhI, cbhII, egI, egII, egIII, egIV, egV, egVI, man1, bglI*)					*Hj*AA9A and 9A-N (ΔCBM) from *H. jecorina* (Hansson et al., 2017; Pierce et al., 2017a); *Mt*AA9A (MYCTH_112089), *Mt*AA9B (MYCTH_80312, also *Mt*LPMO9B) and *Mt*AA9F (MYCTH_92668) variants from *M. thermophila* (Pierce et al., 2017b)
	M. thermophila C1 LC	Extracellular	pPchil(1.8)-Tcbhl NotI	Native	Genomic DNA	*Mt*AA9B (MYCTH_80312, also *Mt*LPMO9B), *Mt*AA9D (MYCTH_92668, also *Mt*LPMO9A), *Mt*AA9E (MYCTH_85556, also *Mt*LPMO9A) and *Mt*AA9W (MYCTH_100518, also *Mt*LPMO9C) from *M. thermophila* (Frommhagen et al., 2016; Frommhagen et al., 2015; Frommhagen et al., 2018)
	N. crassa	Extracellular	pCSR-1	Native	Genomic DNA	*Nc*AA9A, 9B, 9C, 9D, 9E, 9F and 9G from *N. crassa* (Vu et al., 2014a); *Mt*AA9A (MYCTH_112089) and *Mt*AA9D (MYCTH_92668) from *M. thermophila* (Vu et al., 2014a)
	P. verruculosum B1-537 (Δ*niaD*)	Extracellular	modified pUC19	Native or *Pv*CBHI	Genomic DNA	*Hj*AA9A from *H. jecorina* (Bulakhov et al., 2016); *Pv*AA9A from *P. verruculosum* (Semenova et al., 2019)
AA9	*Yeast expression systems*					
	P. pastoris X-33	Extracellular	pPICZα A	α-mating factor	Synthetic cDNA, codon-optimized	*Nc*AA9C, 9E, 9F and 9J from *N. crassa* (Kittl et al., 2012);
				Native and α-mating factor	Synthetic cDNA, codon-optimized	*Gc*AA9A, 9B and 9C from *G. candidum* (Ladevèze et al., 2017)
	P. pastoris KM71H	Extracellular	pPICZα A	α-mating factor	cDNA	*Pc*AA9D from *P. chrysosporium* (Westereng et al., 2011); *Gt*AA9A-2 from *Gloeophyllum trabeum* (Kojima et al., 2016)
	P. pastoris SMD1168H	Extracellular	pPICZα A	Native	cDNA	*Mc*AA9A, 9B, 9F and 9H from *Malbranchea cinnamomea* (Hüttner et al., 2019)
	P. pastoris SuperMan$_5$	Extracellular	pPICZα A	Native	Synthetic cDNA, codon-optimized	*Nc*AA9D from *N. crassa* (O'Dell et al., 2017)
	P. pastoris CBS7435	Extracellular	pPpT4	Native, *Pc*AA9D or α-mating factor	Synthetic cDNA, codon optimized	*Hj*AA9A from *H. jecorina* (Tanghe et al., 2015)
	P. pastoris PichiaPink Strain 4	Extracellular	pPink-GAP-HC	Native	Synthetic cDNA, codon-optimized	*Nc*AA9A, 9C-N and 9D from *N. crassa* (Borisova et al., 2015; Petrović et al., 2019); *Fg*AA9A from *Fusarium graminearum* (Nekiunaite et al., 2016b)
	Y. lipolytica JMY1212 (Zeta)	Extracellular	JMP62UraTEF, JMP62UraTB1his	Native	cDNA	*Hj*AA9A from *H. jecorina* (Guo et al., 2017)
AA10	*Bacterial expression system*					
	E. coli BL21 Star(DE3)	Periplasmic	pRSET B	Native	Genomic DNA	*Sm*AA10A (CBP21) from *S. marcescens* (Vaaje-Kolstad et al., 2005)
	E. coli BL21 Star(DE3)	Periplasmic	pRSET B	*Sm*AA10A	Synthetic DNA, codon-optimized	*Sc*AA10B, 10C and 10C-N from *Streptomyces coelicolor* (Forsberg et al., 2014a; Forsberg et al., 2014b)
	E. coli BL21 Star(DE3)	Periplasmic	pRSET B	*Sm*AA10A	Genomic DNA	*Ef*AA10A from *Enterococcus faecalis* (Vaaje-Kolstad et al., 2012) *Tf*AA10A and 10B-N from *T. fusca* (Forsberg et al., 2014a; Forsberg et al., 2014b)
	E. coli BL21(DE3)	Periplasmic	pET-11a	pelB	Synthetic DNA, codon-optimized	*Ba*AA10A from *B. amyloliquefaciens* (Hemsworth et al., 2013b)
	E. coli BL21(DE3)-RIL	Periplasmic	pET-26b variant	pelB	Genomic DNA	*Sli*AA10B and 10E from *S. lividans* (Chaplin et al., 2016)
	E. coli BL21(DE3)	Periplasmic	pET-28a variants	SacB, pelB, TorA, WompA, OmpASIL2, LM-SEA, LSEA-mut, Exyl, gIII, STII, XCs, and CBHI	Genomic DNA	*Sm*AA10A from *S. marcescens* (Yang et al., 2017)

(*continued on next page*)

Table 1 (*continued*)

CAZy family	Expression strain	Localization	Expression vector	Secretion signal	Gene source	Examples
	E. coli RV308	Periplasmic	pJB	Native and *Sm*AA10A	Genomic DNA or Synthetic DNA, codon-optimized	*Bl*AA10A from *B. licheniformis*, *Cj*AA10A from *Cellvibrio japonicus*, *Jd*AA10A-N from *Jonesia denitrificans*, *Ma*AA10B-N from *Micromonospora aurantiaca*, *Sc*AA10C from *S. coelicolor* and *Sm*AA10A from *S. marcescens* (Courtade et al., 2017)
	Tig Chaperone *E. coli*	Periplasmic	pET-22b	pelB	Synthetic DNA, codon-optimized	*Tt*AA10A-N from *T. turnerae* (Fowler et al., 2019)
	E. coli Rosetta(DE3)	Cytoplasmic	pET-32 Xa/LIC	None	Synthetic DNA, codon-optimized	*Sc*AA10C from *S. coelicolor* (Forsberg et al., 2011)
	E. coli BL21(DE3)	Cytoplasmic	pET-28a(+)	None	Genomic DNA	*Hc*AA10-2 from *Hahella chejuensis* (Ghatge et al., 2014)
			pET-46 Ek/LIC	None	Genomic DNA	*Lm*AA10 from *Listeria monocytogenes* (Paspaliari et al., 2015)
			pET-SUMO	None	Synthetic DNA, codon-optimized	*Ba*AA10A from *B. amyloliquefaciens* (Gregory et al., 2016)
	B. subtilis LKS87	Extracellular	pUBRTA	Native	Genomic DNA	*Bat*AA10 from *B. atrophaeus* (Yu et al., 2016)
	S. elongatus UTEX 2973	Extracellular	pDF-trc	Native and TorA	Synthetic DNA, codon-optimized	*Tf*AA10A from *T. fusca* (Russo et al., 2019)
AA10	*Expression in insect host*					
	Melolontha melolontha	Intracellular, as viral spindles	Not applicaple	Native	Genomic DNA	*Melolontha melolontha* entomopoxvirus (MMEV) fusolin (Chiu et al., 2015)
	Anomala cuprea	Intracellular, as viral spindles	Not applicaple	Native	Genomic DNA	*Anomala cuprea* entomopoxvirus (ACEV) fusolin (Chiu et al., 2015)
	Wiseana spp.	Intracellular, as viral spindles	Not applicaple	Native	Genomic DNA	*Wiseana* entomopoxvirus (WEV) fusolin (Chiu et al., 2015)
AA10	*Expression in plants*					
	Gossypium hirsutum 'Coker 312'	Secreted	pMDC32	Native	Genomic DNA	*Tm*AA10A from *Tectaria macrodonta* (Shukla et al., 2016)
AA11	*Bacterial expression system*					
	E. coli BL21 Star(DE3)	Periplasmic	pET-26a	pelB	Synthetic cDNA, codon-optimized	*Ao*AA11 from *A. oryzae* (Hemsworth et al., 2014)
			pET-26b(+)	pelB	Synthetic cDNA, codon-optimized	*Ff*AA11 and *Ff*AA11-N from *F. fujikuroi* (Wang et al., 2018)
AA13	*Fungal expression systems*					
	A. oryzae JaL355	Extracellular	pAILo2	Native	Genomic DNA	*An*AA13 from *A. nidulans* (Lo Leggio et al., 2015)
	A. oryzae BECh2	Extracellular	pMStr57	Native	cDNA	*Ao*AA13 from *A. oryzae* (Lo Leggio et al., 2015)
	N. crassa	Extracellular	pCSR-1	Native	Genomic DNA	*Mt*AA13 from *M. thermophila* (Vu et al., 2014b); *Nc*AA13 from *N. crassa* (Vu et al., 2014b)
AA13	*Yeast expression system*					
	P. pastoris X-33	Extracellular	pPICZα A	α-mating factor	Synthetic cDNA, codon-optimized	*At*AA13A from *Aspergillus terreus* (Nekiunaite et al., 2016a); *Mo*AA13A from *Magnaporthe oryzae* (Nekiunaite et al., 2016a)
AA14	*Yeast expression system*					
	P. pastoris X-33	Extracellular	pPICZα A	Native	Synthetic cDNA, codon-optimized	*Pc*AA14A and 14B from *Pycnoporus cinnabarinus* (Couturier et al., 2018)
AA15	*Bacterial expression system*					
	E. coli Rosetta 2(DE3)pLysS	Periplasmic	pET-26b	pelB	cDNA	*Td*AA15A and 15B from *T. domestica* (Sabbadin et al., 2018)
AA16	*Yeast expression system*					
	P. pastoris SuperMan$_5$	Extracellular	pPICZα A	Native	Synthetic DNA, codon-optimized	*Aa*AA16 from *Aspergillus aculeatus* (Filiatrault-Chastel et al., 2019)

Strain abbreviations: *A. nidulans*, *Aspergillus nidulans*; *A. oryzae*, *Aspergillus oryzae*; *B. amyloliquefaciens*, *Bacillus amyloliquefaciens*; *B. atrophaeus*, *Bacillus atrophaeus*; *B. licheniformis*, *Bacillus licheniformis*; *B. subtilis*, *Bacillus subtilis*; *E. coli*, *Escherichia coli*; *F. fujikuroi*, *Fusarium fujikuroi*; *G. candidum*, *Geotrichum candidum*; *H. jecorina*, *Hypocrea jecorina*; *M. thermophila*, *Myceliophthora thermophila*; *N. crassa*, *Neurospora crassa*; *P. chrysosporium*, *Phanerochaete chrysosporium*; *P. pastoris*, *Pichia pastoris*; *P. verruculosum*, *Penicillium verruculosum*; *S. cerevisiae*, *Saccharomyces cerevisiae*; *S. coelicolor*, *Streptomyces coelicolor*; *S. elongatus*, *Synechococcus elongatus*; *S. lividans*, *Streptomyces lividans*; *S. marcescens*, *Serratia marcescens*; *T. aurantiacus*, *Thermoascus aurantiacus*; *T. domestica*, *Thermobia domestica*; *T. fusca*, *Thermobifida fusca*; *T. reesei*, *Trichoderma reesei*; *T. turnerae*, *Teredinibacter turnerae*; *Y. lipolytica*, *Yarrowia lipolytica*.

CRISPR-Cas technology, fungal systems are more difficult to handle compared to yeast-based expression systems.

Currently, many of the commercially available *P. pastoris* strains (from Thermo Fisher Scientific or BioGrammatics) have been used for LPMO production (Table 1). The *P. pastoris* X-33 (wild-type), KM71H (*arg4*, *aox1::ARG4*), SMD1168H (*pep4*) and SuperMan$_5$ (HIS$^+$) strains have been employed in conjunction with the pPICZα or pGAPZα vectors, for methanol-inducible expression of LPMO genes under the AOX1 promoter or constitutive expression under the GAP promoter, respectively. The pPICZα and pGAPZα vectors contain Zeocin resistance as selection marker and require Zeocin for plasmid propagation in *E. coli* and selection of *Pichia* transformants. Alternative to antibiotics resistance, the auxotrophic *P. pastoris* strains KM71 (*his4*, *arg4*, *aox1::ARG4*) and PichiaPink Strain 4 (*ade2*, *prb1*, *pep4*) have also been used in connection with the pPIC9K and pPink vectors, respectively. Using the adenine auxotrophic PichiaPink Strain 4 in conjunction with the pPink-GAP-HC plasmid developed by Várnai et al. (2014) is characterized by a simple, color-based selection of successful transformants and constitutive expression of LPMO genes under the GAP promoter. The pPink-GAP-HC vector requires ampicillin for plasmid propagation in *E. coli* and selection of *Pichia* transformants for wild-type mutants using ADE2 complementation. Recently, Guo et al. (2017) engineered an LPMO originating from *H. jecorina* (*T. reesei*) into the non-cellulolytic yeast *Yarrowia lipolytica* JMY1212 (Zeta) as well as a cellulolytic *Y. lipolytica* variant expressing the *T. reesei* cellulases *Tr*Cel7A, *Tr*Cel6A, *Tr*Cel7B and *Tr*Cel5A under the constitutive pTEF promoter. *Y. lipolytica* could produce a functional LPMO at a good yield, 52 mg/L, in spite of hyper-glycosylating the protein (see also the Section 3.3 on Post-translational modifications). Of note, *Y. lipolytica* has been selected as production host of LPMO primarily to improve the cellulolytic ability of a strain engineered for consolidated bioprocessing, thus improving its potential for use in the biorefinery industry.

There is little variation in the strategies of protein production among other LPMO families; fungal AA13 LPMOs have been produced in filamentous fungi *A. oryzae* and *N. crassa*, fungal AA14 and AA16 LPMOs in *P. pastoris*. This could be partly attributed to the limited number of members characterized from these LPMO families. In addition, there are examples of producing eukaryotic LPMOs in a bacterial system: AA11 LPMOs from *A. oryzae* and *Fusarium fujikuroi* and an AA15 LPMO from the insect *Thermobia domestica* have been successfully produced in *E. coli* via periplasmic expression, in a functional form (Hemsworth et al., 2014; Sabbadin et al., 2018; Wang et al., 2018). In case of viruses, which require a host organism to replicate or produce their proteins, LPMOs have been isolated from their natural hosts. Chiu et al. (2015) have produced three viral AA10 LPMOs (fusolins) by infecting *Melolontha melolontha* and *Wiseana* spp. insect larvae with insect poxviruses and subsequently isolating cross-linked LPMO crystals in the form of viral spindles.

In the following sections, we will discuss how the choice of expression host can affect the steps of cloning and expression processes and provide an overview of solutions that are currently in use for the production of these particular enzymes in functional form.

3.2. Gene design and N-terminal processing of LPMOs

3.2.1. The choice of secretion signal and the efficiency of its processing

In eukaryotes, the coding genetic material (exons) is interspaced with stretches of non-coding DNA (i.e. introns). Exon-intron recognition (i.e. splicing signals) may be specific to phyla or even to classes and species (Kupfer et al., 2004). Therefore, often cDNA is used as a template for heterologous expression to avoid introduction of deletions, insertions, or frameshift from misrecognition of intron–exon junctions during transcription or simply to study alternative splicing of the same gene (Kojima et al., 2016). The template DNA is obtained either by rapid amplification of cDNA from the total RNA isolated from the native host using gene-specific primers (Kojima et al., 2016) or by gene synthesis (Petrović et al., 2018). In the latter case, the gene is designed based on the protein sequence (hence it is intron-free) and the codons encoding each amino acid with the highest frequency by the intended expression host are selected to avoid rare codons that may slow down translation. The chance of successful protein expression can be, in some cases, increased further by using codon harmonization. This entails that degenerate codons (i.e. codons encoding the same amino acid) are selected to match their occurrence frequency in the expression host to that in the native strain. This way, the relative speed of translation of subsequent amino acids will be similar to that in the native host (Mignon et al., 2018). Recently, Jacobs and Shakhnovich (2017) have shown that slowly translated codons may be associated with co-translational folding intermediates, the formation of which is essential for proper protein folding. Gene synthesizing companies (e.g. GenScript; Invitrogen GeneArt Gene Synthesis by Thermo Scientific; Genewiz) offer optimization of genes of interest for secretion in various host organisms, including *P. pastoris* and *E. coli*. While co-optimization of a gene for multiple expression strains is a possibility when testing of multiple expression hosts is desired, it often results in suboptimal translation efficiency and may negatively affect protein yield.

LPMOs are unusual enzymes in the sense that their N-terminus takes part in forming the active site. This distinct feature dictates that the N-terminus needs to be processed precisely to obtain a functional LPMO. In most organisms, this implies extracellular secretion, guided by a signal peptide. In the case of Gram-negative bacteria, which have two cell membranes, such as *E. coli*, exporting the protein of interest through the inner membrane only, i.e. to periplasmic space, leads already to the cleavage of the signal peptide (Mergulhão et al., 2005). The major advantage of periplasmic expression over extracellular expression is that overexpression in the periplasmic space allows for recovering a concentrated solution of protein even in case of low or moderate expression and offers comparatively easy protein recovery, using osmotic shock, without the need for a time-consuming ultrafiltration step for upconcentration of the culture broth prior to protein purification. For periplasmic expression of LPMOs in *E. coli*, pelB, other host-specific signal peptides (Chaplin et al., 2016; Yang et al., 2017), the native signal peptide (Mekasha et al., 2016), or a grafted signal peptide from another LPMO (Courtade et al., 2017; Forsberg et al., 2014a) have been used as a leader peptide (Table 1). There are indications in the literature that Sec-targeting signal peptides specific to species that are phylogenetically closer to *E. coli* are processed more accurately than native signal peptides. As an example, Yang et al. (2017) have compared the accumulation of *Sm*AA10A in the cytosol and periplasmic space of *E. coli* BL21(DE3) during expression using thirteen different signal peptides (including the native one) and found that, in this expression system, PelB is, by far, the most efficient in translocating *Sm*AA10A from the cytosol to the periplasmic space. In another study, Courtade et al. (2017) have expressed the AA10 domain of four LPMOs in *E. coli* RV308 using the XylS/*Pm* regulator/promoter system and found that using the signal peptide of *Sm*AA10A outperformed the native signal peptides of three LPMOs from Gram-positive bacteria as well as that of *Cj*AA10A from the Gram-negative bacterium *C. japonicus*. The signal peptide of *Sm*AA10A (CBP21) from the Gram-negative bacterium *S. marcescens* has regularly been used for secretion of AA10 LPMOs instead of the native signal peptide (Courtade et al., 2017; Forsberg et al., 2014b) because *S. marcescens* belongs to the same order, Enterobacterales, as *E. coli*, enabling the recognition and correct processing of this signal peptide by *E. coli*. The signal peptide of *Sm*AA10A has been observed to be cleaved exclusively adjacent to the His1 (unpublished data by Forsberg et al.) and to enable much more efficient translocation of the proteins to the periplasmic space (Courtade et al., 2017). Using non-native signal peptide can be beneficial when expressing LPMOs from Gram-positive bacteria, such as *Bacillus* (Hemsworth et al., 2013b), *Streptomyces* (Courtade et al., 2017; Forsberg et al., 2014a), and *Micromonospora* (Courtade et al., 2017; Forsberg et al., 2018) species, or eukaryotes (Hemsworth et al., 2014).

As an alternative to protein secretion, the N-terminal His of LPMOs required for catalytic activity can be obtained by intracellular expression, by fusing the LPMO to an N-terminal protein tag that can be cleaved off specifically adjacent to the His1. As an example, an AA10 LPMO from *Bacillus amyloliquefaciens* has been expressed intracellularly in *E. coli* being fused to an N-terminal SUMO tag, yielding a functional protein after specific cleavage of the tag adjacent to the LPMO domain's active site His1 by SUMO protease treatment (Gregory et al., 2016).

In eukaryotic expression systems, LPMOs are secreted into the extracellular matrix either by using the native signal peptide or a host-specific secretion signal. When expressing in *P. pastoris* using the pPICZα or pGAPZα vectors, recombinant LPMOs are normally expressed as fusion proteins to an N-terminal peptide encoding the *Saccharomyces cerevisiae* α-mating factor secretion signal. In this case, the gene encoding the mature LPMO protein (i.e. without the signal peptide, having the catalytic His at the N-terminus) is inserted into the multiple cloning site directly after the Kex2 cleavage site. In a different strategy, the pPICZα vectors have also been used for expressing LPMOs with their native signal peptide, by cleaving the vectors with the *Bst*BI restriction, which removes the built-in α-mating factor secretion signal from the vector (Couturier et al., 2018; Hüttner et al., 2019; Kittl et al., 2012) and the preceding Kozak-sequence (Kozak, 1986). In yeast-based expression systems, a yeast-specific Kozak-sequence is inserted right before the start codon to enhance the efficiency of translation initiation (Kozak, 1986). When expressing in *P. pastoris* using the pPink-GAP-HC vector (Várnai et al., 2014), the gene encoding the target LPMO includes the start codon and the native signal peptide and is inserted after the GAP promoter, adjacent to a Kozak-sequence.

The cleavage of foreign signal peptides by *P. pastoris* seems fairly specific in certain cases despite considerable taxonomic differences; the signal peptide of *Ta*AA9A from *T. aurantiacus* has been reported to be processed correctly in 97% of the protein during expression in PichiaPink Strain 4 (Petrović et al., 2018). Similarly, the native signal peptides of *Hj*AA9A (Tanghe et al., 2015) and *Pa*AA9A (Moreau et al., 2019) have been processed correctly in 100% of the protein in *P. pastoris* CBS7435 and X-33 strains, respectively. Notably, the processability of the signal peptide (native to the recombinant protein or specific to the expression host) varies with the target LPMO, and the cleavage of the native signal peptide has been found much more precise than that of the α-mating factor secretion signal, which relies on the Kex2 protease in the Golgi apparatus, in *P. pastoris* (Ladevèze et al., 2017; Moreau et al., 2019; Tanghe et al., 2015). As an example, Ladevèze et al. (2017) have found that the N-terminus of three AA9 LPMOs from *Geotrichum candidum* has been correctly processed only in less than 5% of the secreted proteins when using the α-mating factor secretion signal, whereas it has been processed correctly in 10-90% of the secreted proteins when using the native signal peptides for expression in *P. pastoris* X-33. Similarly, Tanghe et al. (2015) have found that using the native signal sequence of *Hj*AA9A from *H. jecorina* (or from another LPMO, *Pc*AA9D from *Phanerochaete chrysosporium*) is more suitable than the α-mating factor for both protein secretion and processing of the N-terminus during expression in *P. pastoris* CBS7435, despite being foreign for the yeast. These studies underline the importance to confirm correct processing of the N-terminus of recombinant LPMOs, which is essential both for accurate determination of specific activities (e.g., in (Patel et al., 2016)) and for lowering protein production costs for industrial applications (e.g., in (Moreau et al., 2019)). Of note, an LPMO-like protein *Yl*X325 from *Y. lipolytica* has been reported recently (Labourel et al., 2020), the signal peptide of which, being both yeast- and LPMO-specific, could further improve secretion efficiency of LPMOs in *P. pastoris*.

In fungal expression systems, recombinant LPMOs are expressed via their native signal peptide (Table 1 and Supplementary Table S1). Of note, Semenova et al. (2019) have also tested the signal peptide of the endogenous cellobiohydrolase I from the expression host *Penicillium verruculosum* in addition to the native signal peptide when expressing *Pv*AA9A homologously. Both signal peptides have been processed correctly; the extent of cleavage specificity, however, has not been addressed. The success rate of processing foreign signal peptide in fungal expression systems seems to be even better than in *P. pastoris* when expressing LPMOs from other filamentous fungi: >99% for *Ta*AA9A from *T. aurantiacus* produced in *A. oryzae* (Petrović et al., 2018) and 98.6% for *Mt*AA9J from *M. thermophila* produced in *Aspergillus nidulans* (Kadowaki et al., 2018) have been reported to start with His1. Notably, when characterizing an LPMO, not only the correct processing of the signal peptide but also the intactness of the active site residues, including the N-terminal His, should always be checked, especially when reporting specific activities. Active site residues may suffer from autoxidation during protein production, which further reduces the ratio of inactive LPMOs in the protein preparation (for more details, see Section 3.4 Culturing conditions).

3.2.2. Protein tags

Similarly to other proteins, protein tags have been appended to LPMOs to aid protein identification, purification, or folding. Due to the distinct nature of the N-terminal His coordinating the active-site copper of LPMOs, using protein tags at the N-terminus is discouraged. N-terminal tags (e.g. His_6-tag), however, may be used with caution and only in conjunction with cleavage sites that enable specific proteolytic cleavage of the tag from the recombinant protein exactly before the catalytic His that shall become the N-terminus. Examples of such high-precision proteases include the Factor Xa endoprotease (Forsberg et al., 2011; Ghatge et al., 2014), SUMO protease (Gregory et al., 2016) and EKMax enterokinase (Paspaliari et al., 2015). The most common tag used in bacterial, yeast-based and filamentous fungal expression systems is the C-terminal His_6-tag (Table 1 and Supplementary Table S1). While appending a His_6-tag to the recombinant protein largely simplifies its purification, the His_6-tag has been found to bind copper (Watly et al., 2014), which may interfere with substrate binding, as observed by Moser et al. (2008), redox stability, and characterization of LPMOs, as discussed by Eijsink et al. (2019). Alternatively, Strep-tag II, an eight-amino acid peptide, has been used to purify an AA10 and two AA15 LPMOs using the StrepTrap HP affinity column (GE Healthcare) after periplasmic expression in *E. coli* (Fowler et al., 2019; Sabbadin et al., 2018). In the case of metalloproteins, the use of Strep-tag is recommended as, unlike the His_6-tag, it does not chelate metal ions (Skerra and Schmidt, 2000). In addition to the His_6 and Strep purification tags, the human influenza hemagglutinin (HA) and c-myc epitope tags can be used for detection of recombinant proteins. As an example, Russo et al. (2019) used the HA epitope tag to identify the location of a recombinant LPMO during expression in the cyanobacterium *S. elongatus*.

In summary, the use of no tags, or tags that are inert and/or can be cleaved off, is recommended for the production of functional LPMOs.

3.3. Post-translational modifications (PTMs) and protein folding

PTMs, which are host specific, play a critical role in protein structure, stability, and activity. Therefore, studying PTMs in relation to structure and functionality in native and recombinant LPMOs will enable us to select a suitable expression host when producing LPMOs for various biotechnological applications. Irrespective of the enzyme's origin (in terms of native host and CAZy family), structurally the most important PTM is the formation of disulfide bridges. Disulfide bridges are essential for obtaining the common immunoglobulin-like β-sandwich fold of LPMOs. The LPMO domain of AA9s, including *Hj*AA9A (PDB ID, 5O2W), *Ls*AA9A (PDB ID, 5ACG) and *Pc*AA9D (PDB ID, 4B5Q), contains one fully conserved disulfide bridge, which stabilizes the immunoglobulin-like β-sheet core. Interestingly, the LPMO domain of several AA9s, including the two-domain LPMOs *Nc*AA9A (PDB ID, 5FOH) and *Nc*AA9C (PDB ID, 4D7U) as well as many single-domain LPMOs including *Nc*AA9D (PDB ID, 4EIR), *Nc*AA9F (PDB ID, 4QI8),

*Nc*AA9M (PDB ID, 4EIS) and *Tt*AA9E (PDB ID, 3EII) ends with a Cys, forming a second disulfide bridge. The prevalence of this second disulfide bridge among AA9 LPMOs, irrespective of domain structure and regioselectivity, indicates a role of this disulfide bridge in the stabilization of the C-terminus rather than in functionality. Recently, Laurent et al. (2019) have shown that truncation of the linker right after the C-terminal Cys of the LPMO domain of *Nc*AA9C reduces protein stability, most likely by hindering the formation of this disulfide bridge. Moreover, they have suggested that some disulfide bridges may have a role in LPMO specificity as a small subset of AA9 LPMOs contain conserved Cys residues in the L2, L3 and LS loops. This, however, needs further investigation. According to current knowledge, AA11 LPMO domains are stabilized by three disulfide bridges (Hemsworth et al., 2014), while AA15 LPMOs putatively contain five conserved disulfide bridges (Sabbadin et al., 2018). Of the AA10 LPMOs, many contain two disulfide bridges, such as *Tf*AA10A (PDB ID, 5UIZ), *Sc*AA10C (PDB ID 4OY7) and *Jd*AA10A (PDB ID, 5AA7). All cellulose-active AA10s with resolved structure feature two disulfide bridges, corresponding to the residues Cys48-Cys66 and Cys103-Cys222 in *Sc*AA10C (PDB ID 4OY7). However, several of the chitin-active AA10 LPMOs lack the second (e.g. *Bt*AA10A, PDB ID 5WSZ) or both (e.g. *Ef*AA10A, PDB ID 4A02) of these disulfide bridges. The Cys residues forming the second disulfide bridge, which could potentially stabilize the immunoglobulin-like β-sheet core, are mutated to Ala-Ala/Val pairs in 40% of the LPMOs with resolved structure (e.g. Ala76-Ala190 in *Sm*AA10A, PDB ID 2BEM). In a recent study, Tanghe et al. (2017) have shown for *Sc*AA10C that disulfide bridges prevent irreversible unfolding of the protein after heat treatment and contribute to increased thermostability. The role of the occurrence/absence of these disulfide bridges in relation to the stability, function and biological role of the proteins, however, remains to be investigated.

Recently, a disordered active site has been observed in *Sli*AA10E from *Streptomyces lividans* expressed in *E. coli* (Chaplin et al., 2016) and in *Ao*AA13 from *A. oryzae* expressed in an engineered *A. oryzae* strain (Frandsen et al., 2017). Both studies show the occurrence of the catalytic histidines in two states in the apo-form, i.e. where the copper cofactor is coordinated by either three (both catalytic His) or two nitrogen atoms (only His1). The fact that Chaplin et al. (2016) have observed the disordered active site using electron paramagnetic resonance spectroscopy indicates the role of factors other than soaking conditions in the misfolding of the active site, which happens to various degrees as seen in multiple crystal structures of the same protein by Frandsen et al. (2017). It is noteworthy that a disordered active site has been observed for copper-loaded LPMOs in both studies (Chaplin et al., 2016; Frandsen et al., 2017), which implies that copper loading may not be able to fully restore an LPMO's active site to its functional form once it is misfolded. Improper folding of the active site during protein production is a much more plausible explanation for the occurrence of a disordered active site, which could result in large differences between batches of the same LPMO. While partial misfolding of the active site (80% in *Ao*AA13; PDB: 5T7K (Frandsen et al., 2017)) will decrease the specific activity of the enzyme preparation, it is unlikely that it would account for the complete lack of activity found for this enzyme (Lo Leggio et al., 2015) and perhaps also for other AA13s (Nekiunaite et al., 2016a). A more reasonable explanation for that is hitherto undiscovered substrate preference. While the reason for misfolding of the active site remains unknown and further combined structural and spectroscopic data are needed before further conclusions can be drawn, it is tempting to speculate the role of copper deficiency in the growth medium during overexpression of the proteins.

The PTM that has attracted the most attention in LPMO research so far, on the other hand, is the methylation of the N-terminal His (Quinlan et al., 2011) since it is located at the catalytic site. Notably, methylation of the N-terminal His has been found in LPMOs belonging to various LPMO families, including families AA9 (Quinlan et al., 2011), AA13 (Lo Leggio et al., 2015) and AA16 (Filiatrault-Chastel et al., 2019). Characterization of a multitude of LPMOs produced in various expression hosts has revealed that methylation of His1 is specific to filamentous fungi and does not occur in yeast (Petrović et al., 2018; Tan et al., 2015), bacteria (Forsberg et al., 2014b), plants (Yadav et al., 2019), or insects (Chiu et al., 2015; Sabbadin et al., 2018). Apart from improving redox stability (Petrović et al., 2018) and playing a potential role in substrate binding of LPMOs (Frandsen et al., 2016; Simmons et al., 2017), the importance of methylation of His1 in fungi has not been identified yet (for more details, see Section 2 on the structural features of LPMOs). It is noteworthy that the extent of methylation by filamentous fungi depends not only on the host itself but also on the LPMO (or the DNA sequence encoding the LPMO). As an example, *Ta*AA9A from *T. aurantiacus* has been found fully methylated when expressed in *A. oryzae* (Petrović et al., 2018; Quinlan et al., 2011), while the N-terminal His of *Tt*AA9E from *Thielavia terrestris* has been only partially methylated when expressed in *P. verruculosum* (Bulakhov et al., 2016). Similarly to that in recombinant LPMOs, the N-terminal His of endogenous LPMOs isolated from the native strain can also be in a fully (e.g. in *M. thermophila* (Bulakhov et al., 2016)) or partially methylated form (e.g. in *P. verruculosum* (Semenova et al., 2019)).

Similarly to other lignocellulolytic enzymes, LPMOs may carry *N*- and *O*-glycosylations. *N*-glycosylation of the catalytic domain of fungal LPMOs expressed in filamentous fungi has been described in multiple cases by structural studies (Harris et al., 2010; Karkehabadi et al., 2008; Li et al., 2012; Quinlan et al., 2011). The *N*-glycan found on the LPMO domain of *Nc*AA9M close to the substrate-binding surface has been suggested to potentially interact with the cellulose surface (Li et al., 2012), while *N*-glycans found further away from the substrate-binding surface have been suggested to improve protein solubility (O'Dell et al., 2017). Modular fungal LPMOs, similarly to modular cellulases, encounter *O*-glycosylation in the linker region. Hansson et al. (2017) have demonstrated that the glycosylated linker forms an integral part of the LPMO module in *Hj*AA9A from *H. jecorina* (previously *Tr*AA9A) and the removal of the C-terminal linker and CBM1 leads to reduced activity and binding affinity for a truncated variant of *Hj*AA9A. Substrate binding seems especially important for the redox stability of LPMOs (Courtade et al., 2018; Petrović et al., 2019), which warrants further systematic studies on the impact of glycosylation in native and recombinant LPMOs.

Glycosylations are usually not uniform; the type, length, and heterogeneity of *N*- and *O*-glycans depend on the expression host. The most common glycan form may be identified by crystallography, by the strongest electron density map (O'Dell et al., 2017), while proteomics analyses are used to identify the distribution of glycan forms occurring in the protein (Frommhagen et al., 2016). Sample preparation, however, should always be taken into account before drawing premature conclusions about the position and structure of glycans as in many cases LPMOs are deglycosylated with EndoH or PNGase F prior to crystallization (Karkehabadi et al., 2008; Wu et al., 2013) to improve crystal growth and structure data acquisition (Kim and Leahy, 2013). Systematic studies on the effect of glycosylation on LPMO activity has been lacking in the literature. This is partly due to challenges related to the functional characterization of LPMOs (Eijsink et al., 2019). Based on observations from fungal cellulase research, glycosylation may be linked to the following roles: cellulose binding, protease resistance, thermal stability, pH stability, and solubility improvement, and perhaps also resistance to redox inactivation by free radicals.

Fungal LPMOs are routinely produced in *P. pastoris* (Kittl et al., 2012), which has a distinct glycosylation machinery as compared with filamentous fungi. *P. pastoris* is superior to the most common yeast expression host *S. cerevisiae* since it shows controlled glycosylation compared to the extensive hyperglycosylation that might happen in *S. cerevisiae* (Vieira Gomes et al., 2018). Notably, the extent of glycosylation depends not only on the expression host but also on the individual LPMO, as demonstrated by Kittl et al. (2012) for four AA9

LPMOs from *N. crassa* (*Nc*AA9C, 9E, 9F and 9J) expressed in *P. pastoris*. Recently, glycoengineered *P. pastoris* strains have been developed that append shorter, more uniform glycans on the recombinant protein (Jacobs et al., 2009). Expressing *Nc*AA9D from *N. crassa* in *P. pastoris* SuperMan$_5$ has been shown to enhance crystal quality for crystallographic structure determination (O'Dell et al., 2017). Using another yeast species *Y. lipolytica* (to produce LPMO for consolidated bioprocessing purposes) has led to hyperglycosylation of the secreted LPMO, which could not be removed completely even by Endo H treatment (Guo et al., 2017). However, no effect on the catalytic activity has been reported. For LPMOs expressed in bacteria, where glycosylation occurs although less commonly (Nothaft and Szymanski, 2013), no glycosylations have been reported so far.

Recently, Frandsen et al. (2019) have reported phosphorylation near the putative catalytic site of an unusual AA9 (*Ls*AA9B) from *Lentinus similis* that lacks the His-brace (the His residues are replaced with Arg1 and Asn84) and the active site copper, distinct features of an LPMO. The crystal structure confirmed that the Ser25 of *Ls*AA9B recombinantly produced in *A. oryzae* MT3568 is phosphorylated in 70% of the proteins near the N-terminal Arg, the distance between the phosphorylation and Arg1 being 2.9 Å. However, extracellular phosphorylation in fungi is barely studied, and the potential biological function of phosphorylation, and whether it occurs in the native host *L. similis*, remains unknown.

3.4. The impact of the choice of expression host on the production and properties of LPMOs

While most groups regularly use a single well-developed expression system for the production of LPMOs (or specific LPMO families), expression of LPMO variants in multiple expression systems has been reported in a handful of studies, with varying success (Table 2). Yu et al. (2016) expressed a *Bacillus atrophaeus* LPMO (*Bat*AA10) in two bacterial expression systems (*E. coli* and *B. subtilis*) and have found that expression in the *Bacillus*-based expression system gives four times higher protein yield than expression in *E. coli*. Moreover, secretion of the protein to the extracellular milieu by *B. subtilis* allows easier recovery of the protein (Yu et al., 2016), which could be beneficial for the industrial production of the enzyme. In another study, Rodrigues et al. (2017) have expressed a bacterial LPMO, *Tf*AA10A from *T. fusca*, in *E. coli* and *P. pastoris*. Comparing the activity profile of the two His-tagged enzyme variants (Rodrigues et al., 2017) to that reported by Forsberg et al. (2014a) suggests that both enzyme variants have been expressed in an inactive form, potentially because of incorrect processing of the α-mating factor secretion signal in *P. pastoris* (which has been shown for a number of LPMOs as discussed above) and of the native secretion signal in *E. coli* during expression using autoinduction conditions (as the enzyme remained in the cell pellet after periplasmic extraction). Somewhat similarly, expression of two fungal LPMOs, *Tc*AA9A from *Talaromyces cellulolyticus* and *Ta*AA9A from *T. aurantiacus*, in *E. coli* has resulted in the production of inactive LPMOs by Zhang et al. (2019), which is expected considering that the signal peptides had been replaced by a single Met for cloning. Expression of both LPMOs (individually) using their native signal peptide has been, on the other hand, successful in *H. jecorina*, as confirmed by improved biomass saccharification potential of the crude extract (Zhang et al., 2019).

Notably, using alternate expression systems allows for comparison of recombinant LPMOs in term of post-translational modifications, such as host-specific glycosylation patterns (O'Dell et al., 2017), methylation of the N-terminal His, the correct processing of the signal peptide during secretion, and catalytic performance (Petrović et al., 2018). O'Dell et al. (2017) have compared the recombinant variants of *Nc*AA9D expressed in two *P. pastoris* variants, the wild-type X-33 (PDB ID, 5TKF) and the glycoengineered SuperMan$_5$ producing largely uniform and trimmed glycosylation (PDB ID, 5TKG), in terms of processing of the N-terminus, crystal morphology and diffraction resolution. While the (native) signal peptide has been correctly processed by both expression strains, the shorter and more uniform *N*-glycan residues of the *Nc*AA9D variant expressed in the glycoengineered *P. pastoris* strain enhanced crystal quality without the need for deglycosylation of the protein. In fact, using the glycoengineered *P. pastoris* strain for the production of proteins for structural studies may be a better alternative to trimming glycosylations by deglycosylating enzymes, which may lead to the formation of proteins with reduced solubility (O'Dell et al., 2017). In another landmark study, Petrović et al. (2018) have performed detailed functional characterization of two recombinant variants of the fungal *Ta*AA9A (expressed in *P. pastoris* and *A. oryzae*). The native signal peptide has been cleaved almost completely (in >99% and 97% of the cases, respectively) in both variants, corresponding to the production of catalytically active LPMO variants. Essentially, the two LPMO variants differed in PTMs including glycosylation pattern and methylation at the His1, and concerning the catalytic activity, the expression system has had an impact solely on the redox stability of the protein (for a more detailed comparison, see Section 2).

3.5. Culture conditions

Notably, before 2011, i.e. when the active-site metal of LPMOs was identified (Quinlan et al., 2011), the crystal structure of LPMOs had shown either a lack of an active-site metal, e.g. in *Sm*AA10A from *S. marcescens* (Vaaje-Kolstad et al., 2005), or the presence of another metal in the active site, e.g. in *Hj*AA9B (Karkehabadi et al., 2008). In the case of LPMOs expressed in *E. coli*, such as *Sm*AA10A, the lack of active site metal can be attributed to the use of EDTA (0.5M) in the spheroplast buffer for periplasmic extraction. On the other hand, in the case of fungal LPMOs, such as *Hj*AA9B, it can be attributed to the high concentration (i.e. 10 mM) of $NiCl_2$ used in the crystallization solution. Other possibilities for a lack of metal or wrong metal in LPMO crystal

Table 2
Studies comparing multiple protein expression systems for LPMO production.

LPMO	Expression host	Secretion signal	Observation	Reference
*Bat*AA10	*B. subtilis* LKS87	Native	Higher protein yield and extracellular expression in *B. subtilis*; activity confirmed	(Yu et al., 2016)
	E. coli BL21(DE3)	Native		
*Tf*AA10A	*E. coli* BL21(DE3)	Native	Intracellular accumulation of protein in *E. coli* but successful secretion in *P. pastoris*; LPMO inactive in both cases	(Rodrigues et al., 2017)
	P. pastoris X-33	α-mating factor		
*Ta*AA9A, *Tc*AA9A	*E. coli* BL21(DE3)	None	Intracellular production of inactive proteins in *E. coli* (after replacing the signal peptide with Met); successful production of active LPMOs in *H. jecorina*, shown by increased cellulolytic activity as well as activity on 2,6-DMP of the fungal broth	(Zhang et al., 2019)
	H. jecorina T1	Native		
*Nc*AA9D	*P. pastoris* X-33	Native	N-terminus processed correctly in both variants; expression with trimmed and uniform *N*-glycan in *P. pastoris* SuperMan$_5$ yields crystals with higher quality	(O'Dell et al., 2017)
	P. pastoris SuperMan$_5$ (HIS$^+$)	Native		
*Ta*AA9A	*P. pastoris* PichiaPink Strain 4	Native	Catalytically active LPMO variants with correctly processed N-terminus; methylation at the His1 and better redox stability when expressed in *A. oryzae*	(Petrović et al., 2018)
	A. oryzae JaL250	Native		

structures include insufficient levels of copper in the culture medium, the loss of metal during purification (for example due to pH dependence of metal binding) and/or presence of large amounts of chelating agents or divalent cations other than copper in the crystallization conditions. To ensure that LPMOs carry the active-site copper, LPMOs may be supplemented with copper during enzyme production, i.e. directly in the growth medium (Kittl et al., 2012), during enzyme purification, i.e. by incubation of the purified enzyme with 3-5-fold molar excess (Loose et al., 2014) or stoichiometric addition of Cu(II)SO_4 (Chaplin et al., 2016) followed by desalting, or during the enzymatic reaction, i.e. by adding copper-sulfate directly to the enzyme reaction (Hansson et al., 2017). While all these options work for LPMO characterization studies requiring purified proteins, crude extracts are often used without extensive purification at industrial scale, e.g. for biomass saccharification (Harris et al., 2010). Moreover, acquiring copper in the active site is necessary for correct folding and thermodynamic stability. Removal/absence of the copper from the active site leads to a decrease in melting temperature (Hemsworth et al., 2013b; Kracher et al., 2018; Sabbadin et al., 2018) and, consequently, an increase in the proneness of the protein to inactivation. Therefore, enabling sufficient levels of copper in the fermentation medium is critical for LPMO stability.

When producing LPMOs in bioreactor on minimal medium using *E. coli* (Courtade et al., 2017), yeast (Kittl et al., 2012), or filamentous fungi (Punt et al., 2010), the medium may be supplemented with trace metal solution, including copper, to ensure sufficient amount of copper in the medium (Supplementary Table S1). As an example, when growing *P. pastoris* for LPMO expression, the minimal medium has been supplemented with *Pichia* Trace Metal (PTM_1 or PTM_4) salts solution (Bey et al., 2013; Kittl et al., 2012), as also suggested by Invitrogen's *Pichia* fermentation guidelines. Notably, in some cases, PTM_4 salts solution has been added also to complex media (Buffered minimal glycerol/methanol-complex medium, BMGY/BMMY) in shake flask cultures (Bennati-Granier et al., 2015). Although the concentration of trace metals should be sufficient for the LPMOs to ensure correct folding, it needs to be optimized as excessive amounts of free copper may react with reactive oxygen species present in the fermentation medium, leading to formation of radicals, which can damage the target protein (McMahon et al., 2001) or the expression host itself. Notably, the copper in the active center of LPMOs can be reduced by various non-enzymatic electron donors (Frommhagen et al., 2016; Kracher et al., 2018; Westereng et al., 2015). Compounds with similar effect on LPMOs may be present in the growth medium and could reduce the LPMO active site (as well as H_2O_2). In the absence of substrate, this may lead to autoxidation of the catalytic site (Bissaro et al., 2017; Loose et al., 2018) and production of inactive LPMOs. Partial autoxidation of LPMOs has been reported during enzyme production in yeast (Filiatrault-Chastel et al., 2019) and filamentous fungus (Kadowaki et al., 2018). While there are indications that the extent of autoxidation likely depends on the production scale, type of vessel (shake flask *vs* bioreactor) and the redox stability of the enzyme, the impact of culturing conditions on LPMO stability remains to be investigated. To date, the quantitative means to assess an LPMO's activity are scarce (Eijsink et al., 2019), which makes the estimation of the extent of enzyme inactivation difficult. Moreover, the recent discovery of the H_2O_2-based mechanism of LPMOs (Bissaro et al., 2017) has highlighted the complexity and pitfalls of measuring an LPMO's activity (Bissaro et al., 2018; Kuusk et al., 2018). Until a simple, truly quantitative method for assessing LPMO activity is established, such as the method by Filandr et al. (2020), only limited conclusions can be drawn about the effect of culturing (and, in fact, reaction) conditions on the catalytic intactness of LPMOs.

Apart from trace metals, general guidelines should be followed for selecting the correct growth media components, including selection markers (when applicable), and for deciding whether to supplement growth media with antifoam agents, protease inhibitors, etc. Selection markers are especially important for LPMO production in an *E. coli*-based expression system, as, unlike in the case of Eukaryotic expression hosts, the expression vector carrying the gene of the target LPMO is not incorporated into the host chromosome. Protease inhibitors, on the other hand, can reduce degradation of LPMOs during purification and may be added to the crude enzyme solution after separation from the cell pellet (Forsberg et al., 2011; Moser et al., 2008; Mutahir et al., 2018; Sabbadin et al., 2018). Multi-domain proteins expressed in *E. coli*, such as the tetra-modular *Bc*AA10 characterized by Mutahir et al. (2018) where the interdomain linker is not protected by glycosylation as in eukaryotic systems, are prone to proteolytic cleavage. Last but not least, the composition of growth medium may be considered partly for economic reasons, e.g. for production in bioreactor at large scale, and partly for reducing medium complexity, e.g. for simplifying purification of proteins secreted into the culture broth.

3.6. Production scale, scale-up and industrial production

LPMOs have been produced at various scales as reported in the literature. During initial screening, LPMOs may be expressed using 96-well plates in a high-throughput-like manner (Hansson et al., 2017; Tanghe et al., 2015) or using shake flask cultures. In the next step, selected production strains are grown in shaking flasks, which gives satisfactory protein yields for biochemical characterization purposes (Sabbadin et al., 2018; Vu et al., 2014a), before scaling up to production in bioreactor. Notably, high-throughput screening as well as scale-up require analyses that are simple, quick, and suitable for assessing crude extracts directly and, preferentially, can be applied in a high-throughput manner. Ludwig and co-workers have worked over the years to develop such spectroscopy-based assays to assess enzyme activity (Breslmayr et al., 2019; Breslmayr et al., 2018; Kittl et al., 2012). In addition, determining protein yields is rather straightforward; however, evaluating the production efficiency of LPMOs based on protein yields may be misleading without confirming the intactness of the N-terminus. This has been demonstrated by two studies (Moreau et al., 2019; Tanghe et al., 2015), where LPMO production in bioreactor has been optimized in terms of protein yield and N-terminal processing, as the intactness of the N-terminus is indicative of catalytic functionality. Optimally, protein yield, activity and N-terminal processing may be used complementarily as indicators for evaluating the efficiency of LPMO production.

LPMOs have been produced in shake flask and bioreactor (Supplementary Table S1), depending on the expression system used, the research group, the productivity of the expression strain, and purpose of production (i.e., enzyme characterization or development of enzyme application). While there are some counterexamples using Applikon (Courtade et al., 2017) or Harbinger (Loose et al., 2016) bioreactors, LPMOs have been produced in *E. coli*-based expression systems using primarily shake flask cultures. On the other hand, bioreactors are used extensively by groups expressing LPMOs in *P. pastoris* (Bennati-Granier et al., 2015; Karnaouri et al., 2017; Kittl et al., 2012; O'Dell et al., 2017; Tanghe et al., 2015) or filamentous fungi (Hansson et al., 2017; Harris et al., 2010; Punt et al., 2010; Semenova et al., 2020; Zhang et al., 2019). Production in bioreactor generates larger amounts of enzyme. Production of a large, hence uniform, batch of LPMO in bioreactor may be beneficial for structure determination (Hansson et al., 2017; O'Dell et al., 2017), detailed biochemical characterization (Bennati-Granier et al., 2015; Frommhagen et al., 2015; Hüttner et al., 2019; Loose et al., 2016), and the development of enzyme assays (Kittl et al., 2012; Vuong et al., 2017), while it is necessary for large-scale enzyme applications, such as biomass saccharification (Harris et al., 2010; Zhang et al., 2019) and fiber modification (Moreau et al., 2019; Villares et al., 2017).

Being incorporated in the most recent cellulase cocktails (Johansen, 2016; Merino and Cherry, 2007), enzyme manufacturers produce LPMOs at industrial scale using filamentous fungal expression strains. In order to reach industrial-scale production, protein production must

go through a multi-step scale-up process. Despite the growing number of studies reporting LPMO production at small bioreactor scale, little is known on the effect of production scale and production vessel on LPMO production. Recently, Filiatrault-Chastel et al. (2019) have reported that cultivation of a *P. pastoris* strain expressing *Aa*AA16 from *Aspergillus aculeatus* in shake flask culture has led to the production of inactive recombinant proteins, while scaling up protein production to bioreactor scale has enabled the production of a catalytically active *Aa*AA16, with an intact N-terminus in >90% of the protein. The findings of recent studies reporting optimization of LPMO production in bioreactor (Filiatrault-Chastel et al., 2019; Moreau et al., 2019; Tanghe et al., 2015) indicate that assessing intactness of the N-terminus may give further means to improve large-scale production of LPMOs.

4. Conclusions and perspectives

LPMOs are powerful Carbohydrate-Active enZymes, cleaving polysaccharides (and oligosaccharides) via copper-atom mediated oxidation. Since their discovery, the LPMO field has been expanding and is expected to continue to emerge rapidly. LPMOs have become key components of today's state-of-the-art cellulase cocktails, while LPMOs belonging to new AA families have been discovered in various biological settings. Currently, when our understanding of the redox catalysis and inactivation of LPMOs continues to deepen, more and more focus is directed towards quantitative analysis of LPMOs. In order to exploit their full biotechnological potential and enable kinetic characterization, LPMOs need to be produced in a fully active and stable form. Due to the distinct nature of their catalytic site, it is essential that the N-terminus, forming the catalytic site, is processed correctly and remains intact during expression and purification. Correct processing of the N-terminus largely depends on the expression strategy and the compatibility of the signal peptide, if applied, with the protein secretion system of the expression host. In addition, we predict that a suitable expression host performing PTMs compatible with that of the native host should be selected for optimal protein folding and activity. While so far PTMs of LPMOs have been little studied, PTMs, including glycosylation, phosphorylation and acetylation, have been shown to play various roles in the biological activity of proteins in general.

For biotechnological applications, LPMOs are most likely produced in bacterial (*E. coli*), yeast (*P. pastoris*) or filamentous fungal expression systems, depending on their source of origin. It is essential that growth conditions are optimized for minimizing redox stress and thereby autoxidation of the LPMO's catalytic site. For that, the availability of copper in the growth medium, the avoidance of His-tag, and, in the case of fungal LPMOs, the occurrence of N-terminal methylation are some of the key considerations. Here we provide an overview of the current state of the art in LPMO production and highlight knowledge gaps in the field. As each LPMO is distinct and, hence, will require different expression strategy for optimal yield, this review intends to serve as a guide to successful protein expression in the expanding field of LPMOs.

Supplementary data to this article can be found online at https://doi.org/10.1016/j.biotechadv.2020.107583.

Acknowledgements

This work was funded by the Research Council of Norway, Norway, through the grants Bio4Fuels (grant no. 257622) and FunEnzFibres (grant no. 297907).

References

Aachmann, F.L., Sørlie, M., Skjåk-Braek, G., Eijsink, V.G., Vaaje-Kolstad, G., 2012. NMR structure of a lytic polysaccharide monooxygenase provides insight into copper binding, protein dynamics, and substrate interactions. Proc. Natl. Acad. Sci. U.S.A. 109 (46), 18779–18784.

Aehle, W., Bott, R.R., Nikolaev, I., Scheffers, M., Van Solingen, P., Vroemen, C., 2009. Glucoamylase variants with altered properties. Patent No. WO/2009/048488-A1.

Agger, J.W., Isaksen, T., Várnai, A., Vidal-Melgosa, S., Willats, W.G.T., Ludwig, R., Horn, S.J., Eijsink, V.G.H., Westereng, B., 2014. Discovery of LPMO activity on hemicelluloses shows the importance of oxidative processes in plant cell wall degradation. Proc. Natl. Acad. Sci. U.S.A. 111 (17), 6287–6292.

Bennati-Granier, C., Garajova, S., Champion, C., Grisel, S., Haon, M., Zhou, S., Fanuel, M., Ropartz, D., Rogniaux, H., Gimbert, I., Record, E., Berrin, J.G., 2015. Substrate specificity and regioselectivity of fungal AA9 lytic polysaccharide monooxygenases secreted by *Podospora anserina*. Biotechnol. Biofuels 8, 90.

Bey, M., Zhou, S., Poidevin, L., Henrissat, B., Coutinho, P.M., Berrin, J.G., Sigoillot, J.C., 2013. Cello-oligosaccharide oxidation reveals differences between two lytic polysaccharide monooxygenases (family GH61) from *Podospora anserina*. Appl. Environ. Microbiol. 79 (2), 488–496.

Bissaro, B., Røhr, Å.K., Müller, G., Chylenski, P., Skaugen, M., Forsberg, Z., Horn, S.J., Vaaje-Kolstad, G., Eijsink, V.G.H., 2017. Oxidative cleavage of polysaccharides by monocopper enzymes depends on H_2O_2. Nat. Chem. Biol. 13, 1123–1128.

Bissaro, B., Várnai, A., Røhr, Å.K., Eijsink, V.G.H., 2018. Oxidoreductases and reactive oxygen species in conversion of lignocellulosic biomass. Microbiol. Mol. Biol. Rev. 82 (4) (pii: e00029-18).

Bissaro, B., Streit, B., Isaksen, I., Eijsink, V.G.H., Beckham, G.T., DuBois, J.L., Røhr, Å.K., 2020. Molecular mechanism of the chitinolytic peroxygenase reaction. Proc. Natl. Acad. Sci. U.S.A. 117 (3), 1504–1513.

Borisova, A.S., Isaksen, T., Dimarogona, M., Kognole, A.A., Mathiesen, G., Várnai, A., Røhr, A.K., Payne, C.M., Sørlie, M., Sandgren, M., Eijsink, V.G.H., 2015. Structural and functional characterization of a lytic polysaccharide monooxygenase with broad substrate specificity. J. Biol. Chem. 290 (38), 22955–22969.

Breslmayr, E., Hanžek, M., Hanrahan, A., Leitner, C., Kittl, R., Šantek, B., Oostenbrink, C., Ludwig, R., 2018. A fast and sensitive activity assay for lytic polysaccharide monooxygenase. Biotechnol. Biofuels 11, 79.

Breslmayr, E., Daly, S., Požgajčić, A., Chang, H., Rezić, T., Oostenbrink, C., Ludwig, R., 2019. Improved spectrophotometric assay for lytic polysaccharide monooxygenase. Biotechnol. Biofuels 12, 283.

Bulakhov, A.G., Gusakov, A.V., Chekushina, A.V., Satrutdinov, A.D., Koshelev, A.V., Matys, V.Y., Sinitsyn, A.P., 2016. Isolation of homogeneous polysaccharide monooxygenases from fungal sources and investigation of their synergism with cellulases when acting on cellulose. Biochemistry. Biokhimiia 81 (5), 530–537.

Chaplin, A.K., Wilson, M.T., Hough, M.A., Svistunenko, D.A., Hemsworth, G.R., Walton, P.H., Vijgenboom, E., Worrall, J.A.R., 2016. Heterogeneity in the histidine-brace copper coordination sphere in Auxiliary Activity family 10 (AA10) lytic polysaccharide monooxygenases. J. Biol. Chem. 291 (24), 12838–12850.

Chiu, E., Hijnen, M., Bunker, R.D., Boudes, M., Rajendran, C., Aizel, K., Oliéric, V., Schulze-Briese, C., Mitsuhashi, W., Young, V., 2015. Structural basis for the enhancement of virulence by viral spindles and their in vivo crystallization. Proc. Natl. Acad. Sci. U.S.A. 112 (13), 3973–3978.

Chylenski, P., Bissaro, B., Sørlie, M., Røhr, Å.K., Várnai, A., Horn, S.J., Eijsink, V.G.H., 2019. Lytic polysaccharide monooxygenases in enzymatic processing of lignocellulosic biomass. ACS Catal. 9, 4970–4991.

Courtade, G., Le, S.B., Saetrom, G.I., Brautaset, T., Aachmann, F.L., 2017. A novel expression system for lytic polysaccharide monooxygenases. Carbohydr. Res. 448, 212–219.

Courtade, G., Forsberg, Z., Heggset, E.B., Eijsink, V.G.H., Aachmann, F.L., 2018. The carbohydrate-binding module and linker of a modular lytic polysaccharide monooxygenase promote localized cellulose oxidation. J. Biol. Chem. 293 (34), 13006–13015.

Couturier, M., Ladevèze, S., Sulzenbacher, G., Ciano, L., Fanuel, M., Moreau, C., Villares, A., Cathala, B., Chaspoul, F., Frandsen, K.E., Labourel, A., Herpoel-Gimbert, I., Grisel, S., Haon, M., Lenfant, N., Rogniaux, H., Ropartz, D., Davies, G.J., Rosso, M.N., Walton, P.H., Henrissat, B., Berrin, J.G., 2018. Lytic xylan oxidases from wood-decay fungi unlock biomass degradation. Nat. Chem. Biol. 14 (3), 306–310.

Dotson, W.D., Greenier, J., Ding, H., 2007. Polypeptides having cellulolytic enhancing activity and polynucleotides encoding same. Patent No. US 7,271,244-B2.

Eijsink, V.G.H., Petrović, D., Forsberg, Z., Mekasha, S., Røhr, Å.K., Várnai, A., Bissaro, B., Vaaje-Kolstad, G., 2019. On the functional characterization of lytic polysaccharide monooxygenases (LPMOs). Biotechnol. Biofuels 12 (1), 58.

Filandr, F., Man, P., Halada, P., Chang, H., Ludwig, R., Kracher, D., 2020. The H_2O_2-dependent activity of a fungal lytic polysaccharide monooxygenase investigated with a turbidimetric assay. Biotechnol. Biofuels 13, 37.

Filiatrault-Chastel, C., Navarro, D., Haon, M., Grisel, S., Herpoël-Gimbert, I., Chevret, D., Fanuel, M., Henrissat, B., Heiss-Blanquet, S., Margeot, A., Berrin, J.G., 2019. AA16, a new lytic polysaccharide monooxygenase family identified in fungal secretomes. Biotechnol. Biofuels 12, 55.

Fitz, E., Wanka, F., Seiboth, B., 2018. The promoter toolbox for recombinant gene expression in *Trichoderma reesei*. Front. Bioeng. Biotechnol. 6, 135.

Forsberg, Z., Vaaje-Kolstad, G., Westereng, B., Bunæs, A.C., Stenstrøm, Y., MacKenzie, A., Sørlie, M., Horn, S.J., Eijsink, V.G., 2011. Cleavage of cellulose by a CBM33 protein. Protein Sci. 20 (9), 1479–1483.

Forsberg, Z., Mackenzie, A.K., Sorlie, M., Rohr, A.K., Helland, R., Arvai, A.S., Vaaje-Kolstad, G., Eijsink, V.G.H., 2014a. Structural and functional characterization of a conserved pair of bacterial cellulose-oxidizing lytic polysaccharide monooxygenases. Proc. Natl. Acad. Sci. U.S.A. 111 (23), 8446–8451.

Forsberg, Z., Rohr, A.K., Mekasha, S., Andersson, K.K., Eijsink, V.G., Vaaje-Kolstad, G., Sorlie, M., 2014b. Comparative study of two chitin-active and two cellulose-active AA10-type lytic polysaccharide monooxygenases. Biochemistry 53 (10), 1647–1656.

Forsberg, Z., Bissaro, B., Gullesen, J., Dalhus, B., Vaaje-Kolstad, G., Eijsink, V.G.H., 2018. Structural determinants of bacterial lytic polysaccharide monooxygenase functionality. J. Biol. Chem. 293 (4), 1397–1412.

Fowler, C.A., Sabbadin, F., Ciano, L., Hemsworth, G.R., Elias, L., Bruce, N., McQueen-

Mason, S., Davies, G.J., Walton, P.H., 2019. Discovery, activity and characterisation of an AA10 lytic polysaccharide oxygenase from the shipworm symbiont *Teredinibacter turnerae*. Biotechnol. Biofuels 12, 232.
Frandsen, K.E., Simmons, T.J., Dupree, P., Poulsen, J.C., Hemsworth, G.R., Ciano, L., Johnston, E.M., Tovborg, M., Johansen, K.S., von Freiesleben, P., Marmuse, L., Fort, S., Cottaz, S., Driguez, H., Henrissat, B., Lenfant, N., Tuna, F., Baldansuren, A., Davies, G.J., Lo Leggio, L., Walton, P.H., 2016. The molecular basis of polysaccharide cleavage by lytic polysaccharide monooxygenases. Nat. Chem. Biol. 12 (4), 298–303.
Frandsen, K.E., Poulsen, J.C., Tovborg, M., Johansen, K.S., Lo Leggio, L., 2017. Learning from oligosaccharide soaks of crystals of an AA13 lytic polysaccharide monooxygenase: crystal packing, ligand binding and active-site disorder. Acta Crystallogr. D Struct. Biol. 73 (Pt 1), 64–76.
Frandsen, K.E.H., Tovborg, M., Jørgensen, C.I., Spodsberg, N., Rosso, M.N., Hemsworth, G.R., Garman, E.F., Grime, G.W., Poulsen, J.N., Batth, T.S., Miyauchi, S., Lipzen, A., Daum, C., Grigoriev, I.V., Johansen, K.S., Henrissat, B., Berrin, J.G., Lo Leggio, L., 2019. Insights into an unusual Auxiliary Activity 9 family member lacking the histidine brace motif of lytic polysaccharide monooxygenases. J. Biol. Chem. 294 (45), 17117–17130.
Frommhagen, M., Sforza, S., Westphal, A.H., Visser, J., Hinz, S.W., Koetsier, M.J., van Berkel, W.J., Gruppen, H., Kabel, M.A., 2015. Discovery of the combined oxidative cleavage of plant xylan and cellulose by a new fungal polysaccharide monooxygenase. Biotechnol. Biofuels 8, 101.
Frommhagen, M., Koetsier, M.J., Westphal, A.H., Visser, J., Hinz, S.W., Vincken, J.P., van Berkel, W.J., Kabel, M.A., Gruppen, H., 2016. Lytic polysaccharide monooxygenases from *Myceliophthora thermophila* C1 differ in substrate preference and reducing agent specificity. Biotechnol. Biofuels 9 (1), 186.
Frommhagen, M., Westphal, A.H., Hilgers, R., Koetsier, M.J., Hinz, S.W.A., Visser, J., Gruppen, H., van Berkel, W.J.H., Kabel, M.A., 2018. Quantification of the catalytic performance of C1-cellulose-specific lytic polysaccharide monooxygenases. Appl. Microbiol. Biotechnol. 102 (3), 1281–1295.
Garcia-Gonzalez, E., Poppinga, L., Fünfhaus, A., Hertlein, G., Hedtke, K., Jakubowska, A., Genersch, E., 2014. *Paenibacillus larvae* chitin-degrading protein PlCBP49 is a key virulence factor in American Foulbrood of honey bees. PLoS Pathog. 10 (7), e1004284.
Ghatge, S.S., Telke, A.A., Waghmode, T.R., Lee, Y., Lee, K.W., Oh, D.B., Shin, H.D., Kim, S.W., 2014. Multifunctional cellulolytic auxiliary activity protein HcAA10-2 from *Hahella chejuensis* enhances enzymatic hydrolysis of crystalline cellulose. Appl. Microbiol. Biotechnol. 99 (7), 3041–3055.
Gregory, R.C., Hemsworth, G.R., Turkenburg, J.P., Hart, S.J., Walton, P.H., Davies, G.J., 2016. Activity, stability and 3-D structure of the Cu (II) form of a chitin-active lytic polysaccharide monooxygenase from *Bacillus amyloliquefaciens*. Dalton Transactions 45 (42), 16904–16912.
Guo, Z.-P., Duquesne, S., Bozonnet, S., Nicaud, J.-M., Marty, A., O'Donohue, M.J., 2017. Expressing accessory proteins in cellulolytic *Yarrowia lipolytica* to improve the conversion yield of recalcitrant cellulose. Biotechnol. Biofuels 10 (1), 298.
Haacke, A., Fendrich, G., Ramage, P., Geiser, M., 2009. Chaperone over-expression in *Escherichia coli*: apparent increased yields of soluble recombinant protein kinases are due mainly to soluble aggregates. Protein Expr. Purif. 64 (2), 185–193.
Hansson, H., Karkehabadi, S., Mikkelsen, N., Douglas, N.R., Kim, S., Lam, A., Kaper, T., Kelemen, B., Meier, K.K., Jones, S.M., 2017. High-resolution structure of a lytic polysaccharide monooxygenase from *Hypocrea jecorina* reveals a predicted linker as an integral part of the catalytic domain. J. Biol. Chem. 292 (46), 19099–19109.
Harris, P.V., Welner, D., McFarland, K.C., Re, E., Navarro Poulsen, J.-C., Brown, K., Salbo, R., Ding, H., Vlasenko, E., Merino, S., Xu, F., Cherry, J., Larsen, S., Lo Leggio, L., 2010. Stimulation of lignocellulosic biomass hydrolysis by proteins of glycoside hydrolase family 61: Structure and function of a large, enigmatic family. Biochemistry 49 (15), 3305–3316.
Hemsworth, G.R., Davies, G.J., Walton, P.H., 2013a. Recent insights into copper-containing lytic polysaccharide mono-oxygenases. Curr. Opin. Struct. Biol. 23 (5), 660–668.
Hemsworth, G.R., Henrissat, B., Davies, G.J., Walton, P.H., 2014. Discovery and characterization of a new family of lytic polysaccharide monooxygenases. Nat. Chem. Biol. 10 (2), 122–126.
Hemsworth, G.R., Ciano, L., Davies, G.J., Walton, P.H., 2018. Production and spectroscopic characterization of lytic polysaccharide monooxygenases. Methods Enzymol. 613, 63–90.
Hemsworth, G.R., Taylor, E.J., Kim, R.Q., Gregory, R.C., Lewis, S.J., Turkenburg, J.P., Parkin, A., Davies, G.J., Walton, P.H., 2013b. The copper active site of CBM33 polysaccharide oxygenases. J. Am. Chem. Soc. 135 (16), 6069–6077.
Huang, J., Villemain, J., Padilla, R., Sousa, R., 1999. Mechanisms by which T7 lysozyme specifically regulates T7 RNA polymerase during different phases of transcription. J. Mol. Biol. 293 (3), 457–475.
Hüttner, S., Várnai, A., Petrović, D.M., Bach, C.X., Kim Anh, D.T., Thanh, V.N., Eijsink, V.G.H., Larsbrink, J., Olsson, L., 2019. Specific xylan activity revealed for AA9 lytic polysaccharide monooxygenases of the thermophilic fungus *Malbranchea cinnamomea* by functional characterization. Appl. Environ. Microbiol. 85 (23) (pii: e01408-19).
Jacobs, P.P., Geysens, S., Vervecken, W., Contreras, R., Callewaert, N., 2009. Engineering complex-type *N*-glycosylation in *Pichia pastoris* using GlycoSwitch technology. Nat. Protoc. 4 (1), 58–70.
Jacobs, W.M., Shakhnovich, E.I., 2017. Evidence of evolutionary selection for co-translational folding. Proc. Natl. Acad. Sci. U.S.A. 114 (43), 11434–11439.
Johansen, K.S., 2016. Discovery and industrial applications of lytic polysaccharide monooxygenases. Biochem. Soc. Trans. 44 (1), 143–149.
Kadowaki, M.A.S., Várnai, A., Jameson, J.K., Ae, T.L., Costa-Filho, A.J., Kumagai, P.S., Prade, R.A., Polikarpov, I., Eijsink, V.G.H., 2018. Functional characterization of a lytic polysaccharide monooxygenase from the thermophilic fungus *Myceliophthora thermophila*. PLoS ONE 13 (8), e0202148.
Karkehabadi, S., Hansson, H., Kim, S., Piens, K., Mitchinson, C., Sandgren, M., 2008. The first structure of a glycoside hydrolase family 61 member, Cel61B from *Hypocrea jecorina*, at 1.6 A resolution. J. Mol. Biol. 383 (1), 144–154.
Karnaouri, A., Muraleedharan, M.N., Dimarogona, M., Topakas, E., Rova, U., Sandgren, M., Christakopoulos, P., 2017. Recombinant expression of thermostable processive MtEG5 endoglucanase and its synergism with MtLPMO from *Myceliophthora thermophila* during the hydrolysis of lignocellulosic substrates. Biotechnol. Biofuels 10, 126.
Kim, M.S., Leahy, D., 2013. Enzymatic deglycosylation of glycoproteins. Methods Enzymol. 533, 259–263.
Kim, S., Ståhlberg, J., Sandgren, M., Paton, R.S., Beckham, G.T., 2014. Quantum mechanical calculations suggest that lytic polysaccharide monooxygenases use a copper-oxyl, oxygen-rebound mechanism. Proc. Natl. Acad. Sci. U.S.A. 111 (1), 149–154.
Kittl, R., Kracher, D., Burgstaller, D., Haltrich, D., Ludwig, R., 2012. Production of four *Neurospora crassa* lytic polysaccharide monooxygenases in *Pichia pastoris* monitored by a fluorimetric assay. Biotechnol. Biofuels 5 (1), 79.
Kojima, Y., Varnai, A., Ishida, T., Sunagawa, N., Petrović, D.M., Igarashi, K., Jellison, J., Goodell, B., Alfredsen, G., Westereng, B., Eijsink, V.G.H., Yoshida, M., 2016. Characterization of an LPMO from the brown-rot fungus *Gloeophyllum trabeum* with broad xyloglucan specificity, and its action on cellulose-xyloglucan complexes. Appl. Environ. Microbiol. 82 (22), 6557–6572.
Kozak, M., 1986. Point mutations define a sequence flanking the AUG initiator codon that modulates translation by eukaryotic ribosomes. Cell 44 (2), 283–292.
Kracher, D., Scheiblbrandner, S., Felice, A.K., Breslmayr, E., Preims, M., Ludwicka, K., Haltrich, D., Eijsink, V.G.H., Ludwig, R., 2016. Extracellular electron transfer systems fuel cellulose oxidative degradation. Science 352 (6289), 1098–1101.
Kracher, D., Andlar, M., Furtmüller, P.G., Ludwig, R., 2018. Active-site copper reduction promotes substrate binding of fungal lytic polysaccharide monooxygenase and reduces stability. J. Biol. Chem. 293 (5), 1676–1687.
Kupfer, D.M., Drabenstot, S.D., Buchanan, K.L., Lai, H., Zhu, H., Dyer, D.W., Roe, B.A., Murphy, J.W., 2004. Introns and splicing elements of five diverse fungi. Eukaryot. Cell 3 (5), 1088–1100.
Kuusk, S., Bissaro, B., Kuusk, P., Forsberg, Z., Eijsink, V.G.H., Sorlie, M., Valjamae, P., 2018. Kinetics of H_2O_2-driven degradation of chitin by a bacterial lytic polysaccharide monooxygenase. J. Biol. Chem. 293 (2), 523–531.
Labourel, A., Frandsen, K.E.H., Zhang, F., Brouilly, N., Grisel, S., Haon, M., Ciano, L., Ropartz, D., Fanuel, M., Martin, F., Navarro, D., Rosso, M.N., Tandrup, T., Bissaro, B., Johansen, K.S., Zerva, A., Walton, P.H., Henrissat, B., Leggio, L.L., Berrin, J.G., 2020. A fungal family of lytic polysaccharide monooxygenase-like copper proteins. Nat. Chem. Biol. 16 (3), 345–350.
Ladevèze, S., Haon, M., Villares, A., Cathala, B., Grisel, S., Herpoël-Gimbert, I., Henrissat, B., Berrin, J.-G., 2017. The yeast *Geotrichum candidum* encodes functional lytic polysaccharide monooxygenases. Biotechnol. Biofuels 10 (1), 215.
Laurent, C.V.F.P., Sun, P., Scheiblbrandner, S., Csarman, F., Cannazza, P., Frommhagen, M., van Berkel, W.J.H., Oostenbrink, C., Kabel, M.A., Ludwig, R., 2019. Influence of lytic polysaccharide monooxygenase active site segments on activity and affinity. Int. J. Mol. Sci. 20 (24) (pii: E6219).
Levasseur, A., Drula, E., Lombard, V., Coutinho, P.M., Henrissat, B., 2013. Expansion of the enzymatic repertoire of the CAZy database to integrate auxiliary redox enzymes. Biotechnol. Biofuels 6 (1), 41.
Li, X., Beeson, W.T.T., Phillips, C.M., Marletta, M.A., Cate, J.H., 2012. Structural basis for substrate targeting and catalysis by fungal polysaccharide monooxygenases. Structure 20 (6), 1051–1061.
Lo Leggio, L., Welner, D., De Maria, L., 2012. A structural overview of GH61 proteins - fungal cellulose degrading polysaccharide monooxygenases. Comput. Struct. Biotechnol. J. 2 (3), e201209019.
Lo Leggio, L., Simmons, T.J., Poulsen, J.C., Frandsen, K.E., Hemsworth, G.R., Stringer, M.A., von Freiesleben, P., Tovborg, M., Johansen, K.S., De Maria, L., Harris, P.V., Soong, C.L., Dupree, P., Tryfona, T., Lenfant, N., Henrissat, B., Davies, G.J., Walton, P.H., 2015. Structure and boosting activity of a starch-degrading lytic polysaccharide monooxygenase. Nat. Commun. 6, 5961.
Loose, J.S., Forsberg, Z., Fraaije, M.W., Eijsink, V.G.H., Vaaje-Kolstad, G., 2014. A rapid quantitative activity assay shows that the *Vibrio cholerae* colonization factor GbpA is an active lytic polysaccharide monooxygenase. FEBS Lett. 588 (18), 3435–3440.
Loose, J.S., Forsberg, Z., Kracher, D., Scheiblbrandner, S., Ludwig, R., Eijsink, V.G., Vaaje-Kolstad, G., 2016. Activation of bacterial lytic polysaccharide monooxygenases with cellobiose dehydrogenase. Protein Sci. 25 (12), 2175–2186.
Loose, J.S.M., Arntzen, M.O., Bissaro, B., Ludwig, R., Eijsink, V.G.H., Vaaje-Kolstad, G., 2018. Multipoint precision binding of substrate protects lytic polysaccharide monooxygenases from self-destructive off-pathway processes. Biochemistry 57 (28), 4114–4124.
Makinen, S., Juntunen, K., Komander, A., Langfelder, K., Vehmaanpera, J., Puranen, T., 2014. Proteins for the treatment of cellulosic material. Patent No. US/2014/0045225-A1.
McDonald, A.G., Boyce, S., Tipton, K.F., 2009. ExplorEnz: the primary source of the IUBMB enzyme list. Nucleic Acids Res. 37 (Database issue), D593–D597.
McMahon, H.E., Mangé, A., Nishida, N., Créminon, C., Casanova, D., Lehmann, S., 2001. Cleavage of the amino terminus of the prion protein by reactive oxygen species. J. Biol. Chem. 276 (3), 2286–2291.
Mekasha, S., Forsberg, Z., Dalhus, B., Bacik, J.P., Choudhary, S., Schmidt-Dannert, C., Vaaje-Kolstad, G., Eijsink, V.G.H., 2016. Structural and functional characterization of a small chitin-active lytic polysaccharide monooxygenase domain of a multi-modular chitinase from *Jonesia denitrificans*. FEBS Lett. 590 (1), 34–42.
Mergulhão, F.J., Summers, D.K., Monteiro, G.A., 2005. Recombinant protein secretion in *Escherichia coli*. Biotechnol. Adv. 23 (3), 177–202.
Merino, S.T., Cherry, J., 2007. Progress and challenges in enzyme development for

biomass utilization. Adv. Biochem. Eng. Biotechnol. 108, 95–120.
Mignon, C., Mariano, N., Stadthagen, G., Lugari, A., Lagoutte, P., Donnat, S., Chenavas, S., Perot, C., Sodoyer, R., Werle, B., 2018. Codon harmonization–going beyond the speed limit for protein expression. FEBS Lett. 592 (9), 1554–1564.
Moreau, C., Tapin-Lingua, S., Grisel, S., Gimbert, I., Le Gall, S., Meyer, V., Petit-Conil, M., Berrin, J.G., Cathala, B., Villares, A., 2019. Lytic polysaccharide monooxygenases (LPMOs) facilitate cellulose nanofibrils production. Biotechnol. Biofuels 12, 156.
Moser, F., Irwin, D., Chen, S., Wilson, D.B., 2008. Regulation and characterization of *Thermobifida fusca* carbohydrate-binding module proteins E7 and E8. Biotechnol. Bioeng. 100 (6), 1066–1077.
Mutahir, Z., Mekasha, S., Loose, J.S.M., Abbas, F., Vaaje-Kolstad, G., Eijsink, V.G.H., Forsberg, Z., 2018. Characterization and synergistic action of a tetra-modular lytic polysaccharide monooxygenase from Bacillus cereus. FEBS Lett. 592 (15), 2562–2571.
Nekiunaite, L., Isaksen, T., Vaaje-Kolstad, G., Abou Hachem, M., 2016a. Fungal lytic polysaccharide monooxygenases bind starch and beta-cyclodextrin similarly to amylolytic hydrolases. FEBS Lett. 590 (16), 2737–2747.
Nekiunaite, L., Petrović, D.M., Westereng, B., Vaaje-Kolstad, G., Hachem, M.A., Várnai, A., Eijsink, V.G.H., 2016b. *Fg*LPMO9A from *Fusarium graminearum* cleaves xyloglucan independently of the backbone substitution pattern. FEBS Lett. 590 (19), 3346–3356.
Nguyen, H.D., Nguyen, Q.A., Ferreira, R.C., Ferreira, L.C.S., Tran, L.T., Schumann, W., 2005. Construction of plasmid-based expression vectors for Bacillus subtilis exhibiting full structural stability. Plasmid 54 (3), 241–248.
Nothaft, H., Szymanski, C.M., 2013. Bacterial protein N-glycosylation: new perspectives and applications. J. Biol. Chem. 288 (10), 6912–6920.
O'Dell, W.B., Swartz, P.D., Weiss, K.L., Meilleur, F., 2017. Crystallization of a fungal lytic polysaccharide monooxygenase expressed from glycoengineered *Pichia pastoris* for X-ray and neutron diffraction. Acta Crystallogr. Sect. F Struct. Biol. Commun. 73 (Pt 2), 70–78.
Paspaliari, D.K., Loose, J.S., Larsen, M.H., Vaaje-Kolstad, G., 2015. *Listeria monocytogenes* has a functional chitinolytic system and an active lytic polysaccharide monooxygenase. FEBS J. 282 (5), 921–936.
Patel, I., Kracher, D., Ma, S., Garajova, S., Haon, M., Faulds, C.B., Berrin, J.G., Ludwig, R., Record, E., 2016. Salt-responsive lytic polysaccharide monooxygenases from the mangrove fungus *Pestalotiopsis* sp. NCi6. Biotechnol. Biofuels 9, 108.
Petrović, D.M., Bissaro, B., Chylenski, P., Skaugen, M., Sørlie, M., Jensen, M.S., Aachmann, F.L., Courtade, G., Várnai, A., Eijsink, V.G.H., 2018. Methylation of the N-terminal histidine protects a lytic polysaccharide monooxygenase from auto-oxidative inactivation. Protein Sci. 27 (9), 1636–1650.
Petrović, D.M., Várnai, A., Dimarogona, M., Mathiesen, G., Sandgren, M., Westereng, B., Eijsink, V.G.H., 2019. Comparison of three seemingly similar lytic polysaccharide monooxygenases from *Neurospora crassa* suggests different roles in plant biomass degradation. J. Biol. Chem. 294 (41), 15068–15081.
Pierce, B.C., Agger, J.W., Wichmann, J., Meyer, A.S., 2017a. Oxidative cleavage and hydrolytic boosting of cellulose in soybean spent flakes by *Trichoderma reesei* Cel61A lytic polysaccharide monooxygenase. Enzyme Microb. Technol. 98, 58–66.
Pierce, B.C., Agger, J.W., Zhang, Z., Wichmann, J., Meyer, A.S., 2017b. A comparative study on the activity of fungal lytic polysaccharide monooxygenases for the depolymerization of cellulose in soybean spent flakes. Carbohydr. Res. 449, 85–94.
Punt, P.J., Burlingame, R.P., Pynnonen, C.M., Olson, P.T., Wery, J., Visser, J.H., Emalfarb, M.A., Visser, J., Verdoes, J.C., 2010. *Chrysosporium lucknowense* protein production system. Patent No. WO/2010/107303-A3.
Quinlan, R.J., Sweeney, M.D., Lo Leggio, L., Otten, H., Poulsen, J.C., Johansen, K.S., Krogh, K.B., Jorgensen, C.I., Tovborg, M., Anthonsen, A., Tryfona, T., Walter, C.P., Dupree, P., Xu, F., Davies, G.J., Walton, P.H., 2011. Insights into the oxidative degradation of cellulose by a copper metalloenzyme that exploits biomass components. Proc. Natl. Acad. Sci. U.S.A. 108 (37), 15079–15084.
Rantasalo, A., Vitikainen, M., Paasikallio, T., Jäntti, J., Landowski, C.P., Mojzita, D., 2019. Novel genetic tools that enable highly pure protein production in *Trichoderma reesei*. Sci. Rep. 9 (1), 5032.
Rodrigues, K.B., Macêdo, J.K.A., Teixeira, T., Barros, J.S., Araújo, A.C.B., Santos, F.P., Quirino, B.F., Brasil, B., Salum, T.F.C., Abdelnur, P.V., Fávaro, L.C.L., 2017. Recombinant expression of *Thermobifida fusca* E7 LPMO in Pichia pastoris and Escherichia coli and their functional characterization. Carbohydr. Res. 448, 175–181.
Russo, D.A., Zedler, J.A.Z., Wittmann, D.N., Möllers, B., Singh, R.K., Batth, T.S., van Oort, B., Olsen, J.V., Bjerrum, M.J., Jensen, P.E., 2019. Expression and secretion of a lytic polysaccharide monooxygenase by a fast-growing cyanobacterium. Biotechnol. Biofuels 12 (1), 74.
Sabbadin, F., Hemsworth, G.R., Ciano, L., Henrissat, B., Dupree, P., Tryfona, T., Marques, R.D.S., Sweeney, S.T., Besser, K., Elias, L., Pesante, G., Li, Y., Dowle, A.A., Bates, R., Gomez, L.D., Simister, R., Davies, G.J., Walton, P.H., Bruce, N.C., McQueen-Mason, S.J., 2018. An ancient family of lytic polysaccharide monooxygenases with roles in arthropod development and biomass digestion. Nat. Commun. 9 (1), 756.
Semenova, M.V., Gusakov, A.V., Volkov, P.V., Matys, V.Y., Nemashkalov, V.A., Telitsin, V.D., Rozhkova, A.M., Sinitsyn, A.P., 2019. Enhancement of the enzymatic cellulose saccharification by *Penicillium verruculosum* multienzyme cocktails containing homologously overexpressed lytic polysaccharide monooxygenase. Mol. Biol. Rep. 46 (2), 2363–2370.
Semenova, M.V., Gusakov, A.V., Telitsin, V.D., Rozhkova, A.M., Kondratyeva, E.G., Sinitsyn, A.P., 2020. Purification and characterization of two forms of the homologously expressed lytic polysaccharide monooxygenase (*Pv*LPMO9A) from *Penicillium verruculosum*. Biochim. Biophys. Acta Proteins Proteom. 1868 (1), 140297.
Shukla, A.K., Upadhyay, S.K., Mishra, M., Saurabh, S., Singh, R., Singh, H., Thakur, N., Rai, P., Pandey, P., Hans, A.L., Srivastava, S., Rajapure, V., Yadav, S.K., Singh, M.K., Kumar, J., Chandrashekar, K., Verma, P.C., Singh, A.P., Nair, K.N., Bhadauria, S., Wahajuddin, M., Singh, S., Sharma, S., Omkar, Upadhyay, R.S., Ranade, S.A., Tuli, R., Singh, P.K., 2016. Expression of an insecticidal fern protein in cotton protects against whitefly. Nat. Biotechnol. 34 (10), 1046–1051. https://doi.org/10.1038/nbt.3665.
Simmons, T.J., Frandsen, K.E.H., Ciano, L., Tryfona, T., Lenfant, N., Poulsen, J.C., Wilson, L.F.L., Tandrup, T., Tovborg, M., Schnorr, K., Johansen, K.S., Henrissat, B., Walton, P.H., Lo Leggio, L., Dupree, P., 2017. Structural and electronic determinants of lytic polysaccharide monooxygenase reactivity on polysaccharide substrates. Nat. Commun. 8 (1), 1064.
Skerra, A., Schmidt, T.G., 2000. Use of the Strep-Tag and streptavidin for detection and purification of recombinant proteins. Methods Enzymol. 326, 271–304.
Tan, T.C., Kracher, D., Gandini, R., Sygmund, C., Kittl, R., Haltrich, D., Hallberg, B.M., Ludwig, R., Divne, C., 2015. Structural basis for cellobiose dehydrogenase action during oxidative cellulose degradation. Nat. Commun. 6, 7542.
Tandrup, T., Frandsen, K.E.H., Johansen, K.S., Berrin, J.G., Lo Leggio, L., 2018. Recent insights into lytic polysaccharide monooxygenases (LPMOs). Biochem. Soc. Trans. 46 (6), 1431–1447.
Tanghe, M., Danneels, B., Camattari, A., Glieder, A., Vandenberghe, I., Devreese, B., Stals, I., Desmet, T., 2015. Recombinant expression of *Trichoderma reesei* Cel61A in *Pichia pastoris*: optimizing yield and N-terminal processing. Mol. Biotechnol. 57 (11-12), 1010–1017.
Tanghe, M., Danneels, B., Last, M., Beerens, K., Stals, I., Desmet, T., 2017. Disulfide bridges as essential elements for the thermostability of lytic polysaccharide monooxygenase LPMO10C from *Streptomyces coelicolor*. Protein Eng. Des. Sel. 30 (5), 401–408.
Vaaje-Kolstad, G., Houston, D.R., Riemen, A.H., Eijsink, V.G.H., van Aalten, D.M., 2005. Crystal structure and binding properties of the *Serratia marcescens* chitin-binding protein CBP21. J. Biol. Chem. 280 (12), 11313–11319.
Vaaje-Kolstad, G., Westereng, B., Horn, S.J., Liu, Z., Zhai, H., Sørlie, M., Eijsink, V.G.H., 2010. An oxidative enzyme boosting the enzymatic conversion of recalcitrant polysaccharides. Science 330 (6001), 219–222.
Vaaje-Kolstad, G., Bøhle, L.A., Gåseidnes, S., Dalhus, B., Bjørås, M., Mathiesen, G., Eijsink, V.G.H., 2012. Characterization of the chitinolytic machinery of *Enterococcus faecalis* V583 and high-resolution structure of its oxidative CBM33 enzyme. J. Mol. Biol. 416 (2), 239–254.
Vaaje-Kolstad, G., Forsberg, Z., Loose, J.S., Bissaro, B., Eijsink, V.G., 2017. Structural diversity of lytic polysaccharide monooxygenases. Curr. Opin. Struct. Biol. 44, 67–76.
Várnai, A., Tang, C., Bengtsson, O., Atterton, A., Mathiesen, G., Eijsink, V.G.H., 2014. Expression of endoglucanases in *Pichia pastoris* under control of the GAP promoter. Microb. Cell Fact. 13 (1), 57.
Vieira Gomes, A.M., Souza Carmo, T., Silva Carvalho, L., Mendonça Bahia, F., Parachin, N.S., 2018. Comparison of yeasts as hosts for recombinant protein production. Microorganisms 6 (2) (pii: E38).
Villares, A., Moreau, C., Bennati-Granier, C., Garajova, S., Foucat, L., Falourd, X., Saake, B., Berrin, J.G., Cathala, B., 2017. Lytic polysaccharide monooxygenases disrupt the cellulose fibers structure. Sci. Rep. 7, 40262.
Visser, H., Joosten, V., Punt, P.J., Gusakov, A.V., Olson, P.T., Joosten, R., Bartels, J., Visser, J., Sinitsyn, A.P., Emalfarb, M.A., Verdoes, J.C., Wery, J., 2011. Development of a mature fungal technology and production platform for industrial enzymes based on a *Myceliophthora thermophila* isolate, previously known as *Chrysosporium lucknowense* C1. Ind. Biotechnol. 7 (3), 214–223.
Vu, V.V., Ngo, S.T., 2018. Copper active site in polysaccharide monooxygenases. Coord. Chem. Rev. 368, 134–157.
Vu, V.V., Beeson, W.T., Phillips, C.M., Cate, J.H.D., Marletta, M.A., 2014a. Determinants of regioselective hydroxylation in the fungal polysaccharide monooxygenases. J. Am. Chem. Soc. 136 (2), 562–565.
Vu, V.V., Beeson, W.T., Span, E.A., Farquhar, E.R., Marletta, M.A., 2014b. A family of starch-active polysaccharide monooxygenases. Proc. Natl. Acad. Sci. U.S.A. 111 (38), 13822–13827.
Vuong, T.V., Liu, B., Sandgren, M., Master, E.R., 2017. Microplate-based detection of lytic polysaccharide monooxygenase activity by fluorescence-labeling of insoluble oxidized products. Biomacromolecules 18 (2), 610–616.
Walton, P.H., Davies, G.J., 2016. On the catalytic mechanisms of lytic polysaccharide monooxygenases. Curr. Opin. Chem. Biol. 31, 195–207.
Wang, B., Walton, P.H., Rovira, C., 2019. Molecular mechanisms of oxygen activation and hydrogen peroxide formation in lytic polysaccharide monooxygenases. ACS Catal. 9 (6), 4958–4969.
Wang, D., Li, J., Salazar-Alvarez, G., McKee, L.S., Srivastava, V., Sellberg, J.A., Bulone, V., Hsieh, Y.S.Y., 2018. Production of functionalised chitins assisted by fungal lytic polysaccharide monooxygenase. Green Chem. 20 (9), 2091–2100.
Watly, J., Simonovsky, E., Wieczorek, R., Barbosa, N., Miller, Y., Kozlowski, H., 2014. Insight into the coordination and the binding sites of Cu^{2+} by the histidyl-6-tag using experimental and computational tools. Inorg. Chem. 53 (13), 6675–6683.
Westereng, B., Ishida, T., Vaaje-Kolstad, G., Wu, M., Eijsink, V.G.H., Igarashi, K., Samejima, M., Stahlberg, J., Horn, S.J., Sandgren, M., 2011. The putative endoglucanase *Pc*GH61D from *Phanerochaete chrysosporium* is a metal-dependent oxidative enzyme that cleaves cellulose. PLoS ONE 6 (11), e27807.
Westereng, B., Cannella, D., Wittrup Agger, J., Jørgensen, H., Larsen Andersen, M., Eijsink, V.G.H., Felby, C., 2015. Enzymatic cellulose oxidation is linked to lignin by long-range electron transfer. Sci. Rep. 5, 18561.
Westers, L., Westers, H., Quax, W.J., 2004. *Bacillus subtilis* as cell factory for pharmaceutical proteins: a biotechnological approach to optimize the host organism. Biochim. Biophys. Acta 1694 (1), 299–310.
Wong, E., Vaaje-Kolstad, G., Ghosh, A., Hurtado-Guerrero, R., Konarev, P.V., Ibrahim, A.F.M., Svergun, D.I., Eijsink, V.G.H., Chatterjee, N.S., van Aalten, D.M.F., 2012. The *Vibrio cholerae* colonization factor GbpA possesses a modular structure that governs binding to different host surfaces. PLoS Pathog. 8 (1), e1002373.
Wu, M., Beckham, G.T., Larsson, A.M., Ishida, T., Kim, S., Payne, C.M., Himmel, M.E.,

Crowley, M.F., Horn, S.J., Westereng, B., Igarashi, K., Samejima, M., Stahlberg, J., Eijsink, V.G.H., Sandgren, M., 2013. Crystal structure and computational characterization of the lytic polysaccharide monooxygenase GH61D from the Basidiomycota fungus *Phanerochaete chrysosporium*. J. Biol. Chem. 288 (18), 12828–12839.

Yadav, S.K., Archana, Singh, R., Singh, P.K., Vasudev, P.G., 2019. Insecticidal fern protein Tma12 is possibly a lytic polysaccharide monooxygenase. Planta 249 (6), 1987–1996.

Yang, Y., Li, J., Liu, X., Pan, X., Hou, J., Ran, C., Zhou, Z., 2017. Improving extracellular production of *Serratia marcescens* lytic polysaccharide monooxygenase CBP21 and *Aeromonas veronii* B565 chitinase Chi92 in *Escherichia coli* and their synergism. AMB Express 7 (1), 170.

Yu, M.-J., Yoon, S.-H., Kim, Y.-W., 2016. Overproduction and characterization of a lytic polysaccharide monooxygenase in *Bacillus subtilis* using an assay based on ascorbate consumption. Enzyme Microb. Technol. 93-94, 150–156.

Zhang, R., Liu, Y., Zhang, Y., Feng, D., Hou, S., Guo, W., Niu, K., Jiang, Y., Han, L., Sindhu, L., Fang, X., 2019. Identification of a thermostable fungal lytic polysaccharide monooxygenase and evaluation of its effect on lignocellulosic degradation. Appl. Microbiol. Biotechnol. 103 (14), 5739–5750.